

Bioencapsulation Innovations

November 2017

CONTENTS

EDITORIAL	1
XXV Int. Conf. on Bioencapsulation	
BRG GENERAL ASSEMBLY	2
ARTICLE - PONCELET AWARD	
Material science aspects of particle design by spray-drying S. Drusch	4
ARTICLES - BEST STUDENT CONTRIBUTIONS	
Cerasomes for anticancer drug delivery: preparation and in vitro evaluation A. Gileva	6
Polymer-based nanoscale contrast agent encapsulating iodine for X-ray imaging J. Wallyn	8
Encapsulation of pancreatic islet cells for type 1 diabetes treatment C. Bitar	10
Versatile cell microencapsulation platform R. Crouigneau	12
Use of a kenics static mixer for continuous microencapsulation S. Gobert	14
Aroma encapsulation for antibacterial and eco-friendly textile finishing A. Sharkawy	16
Engineering pegylated alginate hydrogels for cell microencapsulation F. Noverraz	18
Development of paromomycin microparticles for cutaneous leishmaniasis treatment A. Matos	20
Evaluation of drug loading in amorphous solid dispersion for efavirenz delivery B. Costa	22
Spheroids versus isolated cells encapsulation for bioartificial liver M. Pasqua	24
Immobilization of probiotic bacteria in biopolymer matrix to increase gastrointestinal survival J. Chanut	26
ASSOCIATION	28

EDITORIAL
XXV INTERNATIONAL CONFERENCE ON BIOENCAPSULATION
La Chapelle sur Erdre, France, July 3-6, 2017


The 25th International Conference on Bioencapsulation has been held close to Nantes, France on July 3 to 6, 2017. The conference venue was exceptional for this special event and the dinner took place in a castle near to one of the nicest rivers of France.



The BRG is now more than 25 years old. Starting from an initiative of seven Canadian researchers, it grown to reach today near to 7000 contacts around the world. From an academic association, it became a research and business network counting 60 % of industrial members.

Over the 25 years, BRG organized 28 international conferences, 25 industrial meetings and conventions, 9 training schools, run three European networks associated to 10 workshops, a total of more than 70 events successfully organized.

BRG also followed the evolution of communication technology. We published the first newsletter in 1992. In 1993, we developed a web site, sharing more and more information. In 1994, communication was performed through mailing list. The first industrial business trade fair was organized in 1996. In 2011, the newsletter turned into electronic format.

In 2017, a mobile app was set up as a future communication tool. In 2018, we will start promoting a data push communication to replace step by step the mailing system. This will be linked to a new version of the web site (<http://bioencapsulation.net>), with a mobile version, but especially to the mobile app (Microencapsulation, available from Apple and Google Play stores). The newsletter will be replaced by weekly or monthly notifications of news and articles.

BRG may then be considered as a real successful network. We wish to thank all the people who contributed to this success. The list would be long and not exhaustive, but let's cite all the local organizers of the different meetings, and all the past and present members of the BRG steering committee. Let's have a special attention to missed Jean-Paul Simon and to still active Ron Neufeld, two pillars of the BRG since its very beginning. We may also cite all the recipients of the Poncelet Award (supported by Procter and Gamble, see photo) who also contributed to BRG activities in the past years.



Twenty-five years means a new generation of members. The future of BRG will be linked to the involvement of new persons in the dynamic of the BRG. We are expecting your participation. If you wish to share the adventure, contact us to know how to help (contact@bioencapsulation.net).

Prof. Denis Poncelet
 BRG President

INTRODUCTION

Each participant of the 25th International conference on Bioencapsulation was invited to attend the 2017 BRG General Assembly, held in La Chapelle sur Erdre, France on July 4, 2017.

2016 ACTIVITY REPORT

Three events were organized by the BRG in 2016:

- 19th Microencapsulation Industrial Symposium, in Frankfurt, Germany on April 4-6, 2016, co-organized with Thorsten Brandau from Brace GmbH.
- 8th Training School on Bioencapsulation in Cork, Ireland on May 30-June 2, 2016, co-organized with Andre Brodkorb, from Teagasc Food Research Center and Joanne Fearon, from University College of Cork.
- 24th International Conference on Bioencapsulation in Lisbon, Portugal on September 21-23, 2016, co-organized with Catarina Pinto Reis, from Lusofona University, and Luis Fonseca, from Instituto Superior Tecnico.

Table 1 reports the participant and contribution numbers for each event. In regards to 2015, the attendance has increased (317 versus 291 participants)

Three issues of the BRG newsletter were published in 2016 under the supervision of Paul de Vos from Groningen University (Netherlands) and edited by Brigitte Poncelet from Impascience (France). The newsletter is sent by email to more than 5000 persons.

- February issue was a collection of papers from industries, especially speakers of the 19th Microencapsulation Industrial Symposium.
- May issue was edited by Amos Nusinovitich, from the Hebrew University of Jerusalem presenting articles related to agriculture.



- The November issue included a contribution from André Brodkorb, 2016 Poncelet award winner, and best student contributions from the 25th International Conference on Bioencapsulation.

Despite the interest for a newsletter, the number of readers is limited. It was decided to make a last issue in November 2017 and then switch to a new communication system (see below communication tools).

2016 FINANCIAL REPORT

The 2016 accounting was externally audited by HPL audit, Nantes, France. A summary of the incomes and expenses is presented in table 2 for each event together with the BRG operating budget. Table 3 presents the cash flow over 2016.

- As usual, the Industrial convention was financially strong, enabling support of other events through grants (19 718 €) and free registration (103 over 317 participants).
- The training school was also financially strong, despite allocation of grants and some free registration, due to a large number of registrations from industry.
- The Lisbon conference was financially balanced.
- The negative balance of the BRG operating activities is due to low membership payment but especially

to expenses linked to the organization of the 2017 events (visit on site, event web pages ...)

- In conclusion, 2016 was a very successful year with regard to attendance, especially from industry. Altogether the cash balance has been increased in 2016 by 40 484 €.

2017-2019 ACTIVITIES

The Steering Committee will be completed with the local organizers for the 2018 and 2019 events.

Four events are being organized in 2017:

- 20th Microencapsulation Industrial Symposium, in Nantes, France in April 10-13, 2017.
- 25th International Conference on Bioencapsulation in La Chapelle sur Erdre, France, in July 3-6, 2017.
- 9th Training School on Microencapsulation in Berlin, Germany on September 11-13, 2017, organized by Stephane Drusch and Anja Maria Oechsle, from TU Berlin.
- 3rd Latin America Symposium on microencapsulation in Pucon, Chile in November 27-29, 2017, organized by Francisca Avecido and Monica Rubikar, from Universidad de La Frontera.

Two events are already planned in 2018:

- 21st Microencapsulation Industrial Symposium, in Montreal, Canada in May 21-24, 2018, co-organized with Corinne Hoesli from McGill Univ..
- 10th Training School on Microencapsulation in Trondheim, Norway, in September 2018, co-organized with Berit Strand and Paul De Vos, supported by Elena Markvicheva, Bart de Haan and Igor Lacik.

It was decided to organize the International Conference on Bioencapsulation biannually and not annually. It was also decided that the Poncelet Award will be given biannually during the International Conference.

Denis Poncelet is developing an online web form for submitting abstracts. The general assembly proposes to limit the abstracts to 1 page. Stephan Drusch and Marijana Dragosavac agreed to be testers of the new system.

For 2019, the following events are in evaluation:

- 26th International Conference on

Table 1 : participation and contributions to the BRG events

	Participants					Contributions		Grants
	Industrials	Reseach.	Students	Exhibitors	Total	Orals	Posters	
Frankfurt	77	13	0	14	104	11	-	12
Cork	20	23	35	-	78	15	-	41
Lisbon	19	55	56	5	135	40	56	50

BRG GENERAL ASSEMBLY

	2016 Frankfurt	2016 Cork	2016 Lisbon	BRG	Total
Registration	144 600 €	28 900 €	48 880 €	630 €	223 010 €
Divers incomes				483 €	483 €
Total recettes	144 600 €	28 900 €	48 880 €	1 113 €	223 493 €
Receptions	73 236 €	11 121 €	21 171 €	1 654 €	107 182 €
Printing-Mailing	10 863 €		3 279 €	99 €	14 241 €
Management	14 610 €	6 720 €	12 409 €	3 240 €	36 979 €
Grant-Missions	2 103 €	5 075 €	12 000 €		19 178 €
Bank costs	1 318 €	82 €	725 €	526 €	2 651 €
Divers			400 €	2 378 €	2 778 €
Total Expenses	102 130 €	22 998 €	49 984 €	7 897 €	183 009 €
Balance	42 470 €	5 902 €	-1 104 €	-6 784 €	40 484 €

European Community. The following persons have shown interest to be involved: Paola Pittia, Paul de Vos, Igor Lacik, Andre Brodkorb, Thierry Vandamme, Catarina Reis, Corinne Hoesli, Marijana Dragosavac.

NEW BRG ADDRESS

The General Assembly was informed that the head office of the BRG association has been moved to :

114 Allée Paul Signac
44240 Sucé sur Erdre.

STEERING COMMITTEE

The General Assembly elected the following Steering Committee, valid until the next General Assembly to be held in September 2019 :

- The only nominee for president was Denis Poncelet from Oniris Nantes, France, and the vote was carried unanimously by the members.
- The only nominee for treasurer was Ron Neufeld from Queen's University Kingston, Canada, and the vote was carried unanimously by the members.
- A request for nominations for secretary was presented, and two persons volunteered, Stephane Drusch from TU Berlin, Germany, and Corinne Hoesli from McGill University Montreal, Canada. A vote was called, and both persons were jointly voted.
- Paul De Vos was re-elected as co-president and as newsletter chief-editor, with support from Brigitte Poncelet.
- Stephan Drusch has been nominated to head the Poncelet award committee.

Bioencapsulation in Italy, co-organized with Paola Pittia from University of Teramo.

- 11th Training Scool on Microencapsulation in Loughborough University, UK, co-organized with Marijana Dragosavac.
- 22nd Microencapsulation Industrial Symposium in Spain, co-organized by Izaskun Maranon, from Tecnalía.

In 2020, the Microencapsulation Industrial Symposium, may be organized in Switzerland with the support of Erbo Spray.

Paul De Vos and Denis Poncelet are developing a mobile application which would be a mirror of a redesigned web site to give quick access to all information.

In parallel, the newsletter will be replaced by news with information from members (short articles, conference announcements, thesis abstract ...). The members will be advised of information through notifications.

A campaign will be run to renew the contact list (7000 contacts but many have to be updated). Paola Pittia, Herley Casanova and Claudia Preininger agreed to help.

To attract a broader industrial interest, a different logo will be used for the industrial convention.

End of 2015	78 770 €
2016 Franckfurt	42 470 €
2016 Cork	5 902 €
2016 Lisbon	- 1 104 €
BRG	- 6 784 €
Balance	40 484 €
End of 2016	119 254 €



COMMUNICATION TOOLS

Due to the amount of spam, communication by emails is no longer efficient. It was decided to promote other communication tools.

NETWORKING

Stephan Drusch has proposed to apply for a RISE project from the European commission. This will allow exchange of students and researchers between groups, inside and outside of the

The Steering Committee will be completed with the local organizers for the 2018 and 2019 events.

CLOSING

Following questions and discussion, the General Assembly was closed.

MATERIAL SCIENCE ASPECTS OF PARTICLE DESIGN BY SPRAY-DRYING

Drusch, S., Technische Universität Berlin, Germany

INTRODUCTION

In the past decade a multitude of review articles on microencapsulation of food ingredients has been published. It is consensus that a wide range of encapsulation techniques may be used and that each technique has specific advantages and limitations resulting from the nature of the encapsulate, the process conditions, the type of carrier matrix suitable for the specific technique and the final application.

Spray drying is frequently described as a technique, which is economically attractive, widely available, offers excellent protective performance and is thus the predominant technique for encapsulation of food ingredients. As a consequence, high expectations with respect to loading capacity, shelf life and the range of applications grew in the food industry twinned with the development of a new generation of highly sensitive ingredients. Together with consumer expectations to have "all natural" products, which limits the range of materials for carrier design, these factors have been the key drivers for systematic research pushing the limits of this encapsulation technique.



THE BASICS

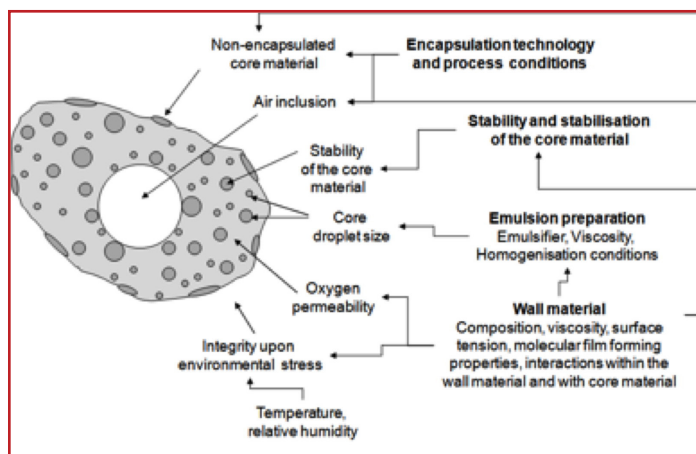
The process of encapsulation by spray-drying comprises the preparation of an aqueous solution of the carrier matrix, dispersion of the encapsulate into the solution, atomisation of the dispersion into the drying chamber and particle generation through evaporation of water from the droplets. As a result a matrix-type particle results with the encapsulate dispersed throughout the solidified carrier matrix. Matrix constituents usually comprise a surface-active constituent for stabilising the liquid dispersion and a bulk constituent. Several aspects of process-structure-

function relationships have been investigated and may be regarded as generally accepted for a wide range of systems.

Among these relationships are:

- Increasing the load of the encapsulate reduces encapsulation efficiency.
- Reduction of the droplet size of the dispersed phase increases encapsulation efficiency.
- Increasing molecular weight of the carrier matrix constituents affects drying kinetics and increases the risk of particle ballooning.
- Low glass transition temperature of the carrier matrix constituents facilitates undesired phase transition of the amorphous matrix and unintended release of the encapsulate

Other issues are less obvious and are discussed below.



Factors determining the stability of lipophilic functional ingredients and interacting product and process characteristics (Drusch et al. 2012)

kinetic stability in the liquid state. As a consequence, surface-activity has initially been in focus when optimizing a formulation. The surface-active ingredient must occupy the newly created interface immediately after its generation before coalescence of the dispersed core material occurs.

Furthermore, excess surface material occupies the droplet surface immediately after atomisation in the drying chamber and may help to modify the surface composition of the spray-dried particle. A less known factor is the viscoelasticity of the interfacial film. Atomisation represents severe mechanical stress for the dispersed core material and high mechanical strength as represented by a high complex viscoelastic modulus of the interfacial film with predominant elastic character is desirable.

Materials science aspects thus play a crucial role in tailoring the oil-water interface. In this context also chemical aspects need to be considered. Protein modification may significantly improve chemical stabilisation of the core material without negatively affecting physical properties of the interfacial film and thus physical structure of the encapsulation system. With quillaja saponins a new functional emulsifying constituent with antioxidative activity for spray-dried encapsulation systems has been



STRUCTURING THE OIL/WATER-INTERFACE

The oil-water-interface is occupied by the surface-active constituent of the carrier matrix. By lowering the interfacial tension it facilitates breakup of the dispersed phase during formation of the dispersion and increases the

described. Depending on their chemical structure, saponins show a very unique behaviour at the interface different from other low molecular weight surfactants and thus encourage more intense research to identify new materials to structure the interface.

PHASE BEHAVIOUR OF THE CARRIER MATRIX CONSTITUENTS

As outlined above, the carrier matrix represents a complex mixture of biopolymers, where compatibility issues may arise. Thermodynamic aspects like the free energy of mixing and intermolecular interactions need to be considered to evaluate the phase behaviour. This knowledge may be used to tailor specific structural elements like e.g. multiple layers of oppositely charged biopolymers to form a dense film covering the encapsulate. Different combinations have been described in the literature in the past years. The range of positively charged biopolymers limits the variability. Furthermore it needs to be considered that during processing, incorporation in a food matrix or in physiological media environmental conditions may significantly change and may affect the specific structure and thus functionality of the carrier matrix. The same holds true for undesired phenomena based on the phase behaviour of mixed biopolymer systems affecting the kinetic stability of the emulsion prior to spray-drying.

The bulk carrier matrix nowadays in the majority of cases still consists of hydrolysed starch. From observations of the impact of the dextrose equivalent on the stability of the encapsulate research activities evolved that resulted in a very good understanding of the impact of molecular weight on the sub-micron structure of the carrier matrix and effects on oxygen permeation and moisture sorption. Data from the literature indicate that on a microstructural level phase separation occurs.

CONCLUSION

Just a few aspects have been outlined above, but these examples already show, that microencapsulation by spray drying well developed from an empirical search of converting an emulsion into a powder with high encapsulation efficiency to an encapsulation technique offering a wide range of

opportunities. Still in a certain range of applications spray-dried particles cannot compete with the functionality of more complex encapsulation techniques with multiple processing steps. But combining the knowledge of materials behaviour with process design nowadays already allows the design of complex heterogeneous structures, which may overcome the limitations frequently associated with spray-dried particles. I am convinced that research in the upcoming years thus will help to develop a new generation of spray-dried particles making it worth to re-visit this encapsulation technique.

REFERENCES

Drusch, S., Regier, M. and Bruhn, M., 2012: Recent advances in the microencapsulation of oils high in polyunsaturated fatty acids. In: McElhatton et al. (Eds.) "Novel technologies in food science - their impact on products, consumer trends and environment. Springer Verlag, Hamburg, Tokio, New York. 159-183.

Acknowledgement

The presenting author gratefully acknowledges the contribution of all collaborators, who are co-authors of the corresponding publications



Prof Stephan Drusch

TU Berlin
Food Technol. & Food Material Sc.
Berlin, Germany
stephan.drusch@tu-berlin.de

Stephan Drusch is Professor for Food Technology and Food Material Science at the Technische Universität Berlin. He studied at the University of Kiel (Diploma, PhD) and worked as a researcher in the dairy industry, at the University of Kiel and the University of Milan. His research activities focus on structure-function relationships in food processing with emphasis on dispersed systems and the encapsulation of food ingredients.

PONCELET AWARD

Since 2011, with the kind sponsorship from Procter & Gamble, an award is attributed to a person having contributed strongly to the development of the microencapsulation. The selection is based on open nomination from all BRG members. A selection committee composed of 4 industrials and 4 scientific researchers analyzes the proposal and makes the final selection.

2017 Poncelet Award has been attributed to Professor Stephan Drusch.



BEST STUDENT CONTRIBUTIONS

The Bioencapsulation Research Group attributed a prize consisting in a diploma and a trophée to 11 best student contributions presented at the annual International Conference. The scientific committee, composed of 15 scientific and industrial members, rated the student contributions, both orals and posters. The final selection is based on the mean of the 15 scores provided by the scientific committee members.



CERASOMES FOR ANTICANCER DRUG DELIVERY: PREPARATION AND IN VITRO EVALUATION

¹ Gileva A., ² Kondrya U., ² Mironova M., ² Sarychev G., ² Budanova U., ² Sebyakin Yu., ¹ Markvicheva E.

INTRODUCTION AND OBJECTIVES

Cerasomes are hybrid organic-inorganic nanoparticles which could be considered as liposomes with very durable silicon shell. However, these nanocarriers are much more stable than liposomes and are promising for prolonged anticancer drug delivery. The aim of the study was to obtain and characterize cerasomes loaded with doxorubicin (DOX) and to evaluate their accumulation and *in vitro* cytotoxicity both in monolayer cell culture (2D) and multicellular tumor spheroids (3D).

MATERIALS & METHODS

Chemicals

Amino acids L-asparaginic acid, L-ornithine, succinic acid, dodecanol-1, (3-aminopropyl)triethoxysilane, dipalmitoyl-phosphatidylcholine (DPPC), doxorubicin hydrochloride, fluorescein isothiocyanate and Hoechst 33258 were from Sigma-Aldrich (Germany). Trypsin-EDTA solution (0.25% v/v), DMSO (99.5%), PBS (pH 7.4), Dulbecco's modified Eagle's medium (DMEM), fetal bovine serum (FBS) were purchased from PAN-Biotech (Germany).



Preparation and characterization of cerasomes

Cerasomes were prepared by modified thin film liposome formation technique. Briefly, synthesized cerasome-forming lipids (CF-lipids) and DPPC (added to several samples) were dispersed in 3 ml of 10% hydrochloric acid solution in ethyl alcohol. The obtained dispersion was stirred at 35°C for 1 h, and then 1.5 ml of chloroform was added. The solution was evaporated to get a thin film which was lyophilized for 6 h. The obtained dry thin film was moistened with a DOX solution (40% w/v) in PBS (pH 7.4). Finally, sonicated cerasomes (30 min, 45°C) were passed through an extruder with a pore

size filter of 400 nm. A drug excess was removed by a dialysis. The cerasomes size was measured by Zetasizer Nano ZS, Malvern (UK). The cerasome stability was studied by spectroscopy at a wavelength of 400 nm (for free cerasomes) and 470 nm (for DOX-loaded vesicles).

Cell culture and tumor spheroid formation

Human breast adenocarcinoma MCF-7 cells were cultivated in DMEM supplemented with 10% FBS in a 5% CO₂ humidified atmosphere at 37°C. The cells were detached after treatment with trypsin-EDTA solution, and the culture medium was replaced every 3-4 days. Tumor spheroids were generated using RGD-induced cell self-assembly platform previously developed at our lab [Akasov R., 2016]. Briefly, cells (50 000 cells/mL) were seeded in a 96-well plate (100 µL/well) and incubated at 37°C for 2-3 h until the cells attached to the plate bottom. Then in each well the medium was replaced with 100 µL of complete DMEM containing cyclo-RGDfK(TPP) peptide (40 µM). Finally, the plate was transferred to a CO₂-incubator, and RGD-induced spheroid formation was observed in 2-3 days.

Confocal microscopy

To prepare samples, DOX-loaded cerasomes were incubated with cell suspension in DMEM in the CO₂-incubator for 15 min and 1 h. To visualize nuclei, the cells were stained with Hoechst (50 µM, 15 min). Then the cells were washed three times with PBS (pH 7.4), fixed with a CC/Mount fluorophor protector and observed by confocal microscopy. Excitation wavelength values were 470 nm for DOX and 360 nm for Hoechst 33258, while fluorescence signals were collected at 560-650 and 380-460 nm for DOX and Hoechst, respectively.

Flow cytometry

For flow cytometry analysis, a BD FACSCalibur fluorescent-activated flow cytometer and BD CellQuest software were used. Cells were seeded in a 24-well plate (50000

cells/well) followed by overnight incubation. Then the culture medium was removed, and free DOX or DOX-loaded cerasomes (suspension in DMEM) were added. After treatment, the cells were washed with PBS (pH 7.4) to remove remaining cerasomes. Cerasome accumulation within the cells was calculated as a ratio cells with cerasomes / cells without cerasomes.



Cytotoxicity study

The cells were seeded in a 96-well plate (5000 cells/well) followed by overnight incubation. Free DOX or cerasomes at various dilutions (10:5; 10:1; 10:0.1; 10:0.01 µMol DOX) were added to each well, and then the cells were transferred to the CO₂-incubator for 24, 48 and 72 h. After treatment, the cells were stained with a 0.05% (w/v) MTT solution in DMEM for 4 h. Then medium was replaced with DMSO (100 µL/well) and an absorbance (570 nm) was measured using Multiskan FC reader (Thermo Scientific, USA). The half maximal inhibitory concentration (IC₅₀) was determined as drug concentration which resulted in 50% inhibition of cell growth.

RESULTS & DISCUSSION

Usually, CF-lipids should contain four main blocks: silicon component (a), linker (b), hydrophilic (c) and hydrophobic (d) domains (Fig. 1).

In this study, two types of CF-lipids based on amino acids and fat alcohols,

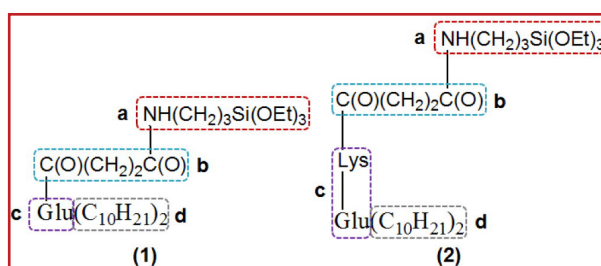


Fig. 1. The structure of synthesized neutral (1) and cationic (2) CF-lipids.

ARTICLE

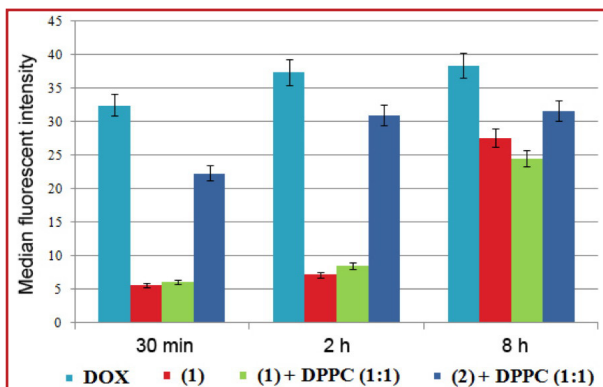


Fig. 2. Accumulation of free DOX and DOX-loaded cerasomes in human breast adenocarcinoma MCF-7 cells. Flow cytometry.

namely neutral lipid (1) and cationic one (2) were synthesized. Both CF-lipids were used for preparation of “pure” (only CF-lipid) or “mixed” (CF-lipid + disintegrating DPPC lipid) cerasomes. Four samples, namely “pure” neutral cerasomes (1), “pure” cationic cerasomes (2), “mixed” neutral cerasomes (1)+DPPC(1:1) and “mixed” cationic cerasomes (2)+DPPC(1:1) were obtained. Some physico-chemical parameters of the cerasomes are listed in Table 1.

Table 1. Physico-chemical parameters of cerasomes

Cerasomes lipid composition	Diameter nm	PI %	ζ -potential mV
(1)	140	99	+11
(2)	180	95	+40
(1) + DPPC (1:1)	230	96	+4

The introduction of free amino group in the cerasome structure was found to lead to approx. 4-fold charge increase, while addition of disintegrating lipid (1:1) caused 1.5-fold diameter enhancement of the obtained nanoparticles. The cerasome charge was double reduced. The DOX encapsulation efficiency was approx. 92% for all cerasomal dispersions. The “pure” cerasomes were stable at least for 120 days, while the “mixed” ones kept stability only for 30 days. Nevertheless, the stability of the «mixed» cerasomes was double higher than that of conventional liposomes.

A quantitative analysis of the cerasome accumulation in the cells (monolayer culture) was performed by flow-cytometry (Fig. 2). Cerasomes with a neutral surface charge (1) and (1)+DPPC(1:1) were accumulated within the cells 5 or 6-fold slower than free DOX. On the other hand, the positive cerasome surface charge provided 4-fold faster penetration the cells. Cerasomes localization was studied by confocal microscopy (Fig. 3).

In case of monolayer culture (2D conditions) the “pure” cerasomes penetrated the cells and localized in the cytoplasm in 15 min, and then accumulated within the ER membrane and other organelles in 1h. In case of tumor spheroids the cerasomes needed approx.

2h to reach the spheroid’s center. Free cerasomes (1) did not show any cytotoxic effect (Fig.4). Although all cerasomes contained similar DOX amounts, IC50 values differed. The biggest cytotoxicity was observed for the (2)+DPPC+DOX “mixed” cationic cerasomes, which could be explained by their higher accumulation in the cells. The cytotoxicity of the “pure” cerasomes was revealed only after 72 h incubation with DOX at concentrations above 5 μ Mol.

CONCLUSIONS AND PERSPECTIVES

Several samples of the “pure” and “mixed” cerasomes were obtained and characterized. The «pure” and “mixed” cerasomes were stable at least for 120

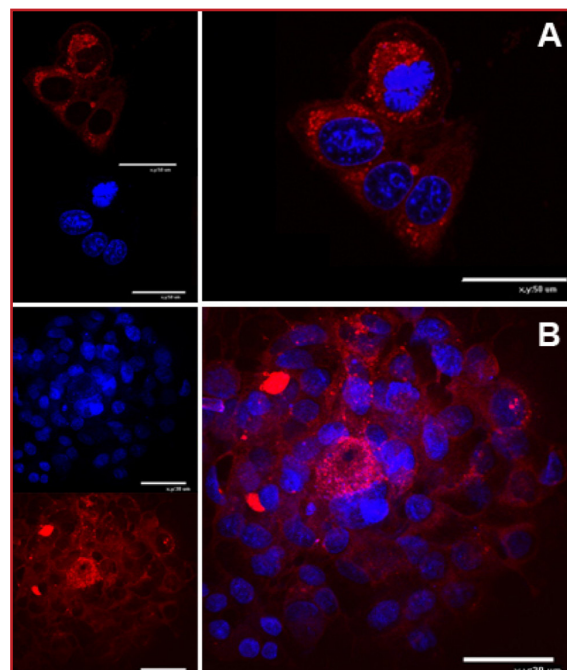


Fig. 3. Confocal images of the “mixed” cationic cerasomes in MCF-7 cells after 1 h incubation with monolayer culture (A) and 2h incubation with tumor spheroids (B). Cell nuclei are stained in blue (Hoechst), the cerasomes are in red (DOX). Scale bar is 50 μ m (A) and 30 μ m (B).

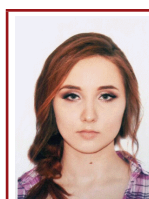
and 30 days respectively. The properties of cerasomes were varied by varying lipid composition. The highest accumulation and cytotoxicity were observed for the “mixed” DOX-loaded cationic cerasomes, while the “pure” cerasomes are promising as sustained drug delivery systems.

REFERENCES

Akasov R. et al. *Int J Pharm*, 2016, 506(1-2):148-57.

Full address

¹Shemyakin–Ovchinnikov Institute of Bioorganic Chemistry RAS, Moscow, Russia
²Moscow Technological University, Moscow, Russia



Anastasia Gileva
Shemyakin–Ovchinnikov Insti. of Bioorg. Chem. RAS, Moscow, Russia
sumina.anastasia.as@gmail.com

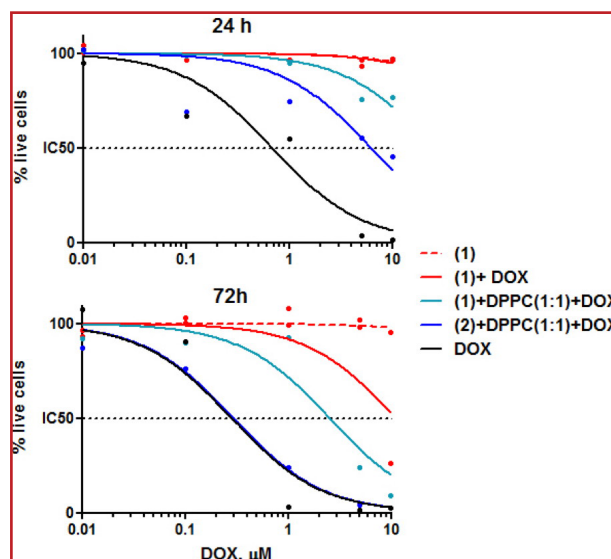


Fig. 4. The viability of MCF-7 cells after 24 h and 72 h incubation with DOX (control) and cerasomes.

POLYMER-BASED NANOSCALE CONTRAST AGENT ENCAPSULATING IODINE FOR X-RAY IMAGING

Wallyn, J., Anton, N., Serra, C., Vandamme, T.F. - University of Strasbourg, France

INTRODUCTION & OBJECTIVES

Nowadays, formulations of contrast agent (CA) for X-ray imaging rely mainly on small hydrosoluble iodinated molecules capable of attenuating X-Ray and providing contrast enhancement in tissues in which they are accumulated. However, these CAs suffer from a lack of long-time retention and fast excretion issues leading to use high doses for a poor efficiency and causing toxic side effects. Literature shows that involving iodinated nanoparticles is one the best alternative to overcome those limitations (Li, 2014). Colloidal polymeric nanoparticles (PNPs), and more precisely those encapsulating iodinated macromolecules, have been reported as very suitable to fulfill those needs. They have been mentioned as i) stable nanocarrier, based on double part nanostructure including a rigid polymeric core and stealth shell, capable of being iii) loaded with high iodine content within the inner core imparting iv) good radiopacity property. Furthermore, PNPs have been pointed out to have v) a controllable size distribution and surface properties. Owing to such tunable design, radiopaque PNPs can be vi) delivered to site of interest and show vii) improved pharmacokinetics profile compared to current clinical CAs abovementioned (El-sabahy, 2015; Fuchs, 2015). Nano-sized biocompatible construct made of iodine-loaded rigid colloids appear though as an efficient and innovating kind of CA for non-invasive diagnostic purpose by X-ray imaging. However, there is still a need to find out compromise between iodine content for strong X-ray attenuation ability and size distribution for a safe *in vivo* administration. Promising assays were obtained from emulsion polymerization of the 2-methacryloyloxyethyl(2,3,5-triiodobenzoate) monomer (MAOTIB) (Galperin, 2007) leading to 30 nm iodinated PNPs accumulated in liver, spleen, lymph nodes and kidneys once intravenously administrated to dog. Consequently, biodistribution remained to improve since: the more different organs accumulate PNPs due to their small size, the less concentrated PNPs are in those compartments, which means that the less the contrast will be significant in each.



Here, we investigated a straightforward approach to produce biocompatible and controllable size distribution polymer-based CA encapsulating radiopaque material. To this end, we applied nanoprecipitation dripping technique (Fessi, 1992) to obtain PEGylated PNPs from a preformed iodinated homopolymer, poly(MAOTIB), synthesized by radical polymerization of the MAOTIB. The strategy applied here was to encapsulate high amount of iodine by grafting it onto the polymer backbone. Nanoprecipitation or solvent displacement method has been reported as very efficient technique to formulate monodisperse and nanoscale colloids by playing on key parameters such as the polymer and surfactant weight ratio. In our case, it appears as the most suitable method to cope with trouble of balancing size distribution and iodine content. In this way, the strength of such PNPs formulation lies not only on its X-Ray attenuation properties but also on the control over the design of PNPs to impart suitable physicochemical features for *in vivo* use. The roles of polymer loaded as a core of nanoconstruct and the surfactant-to-polymer weight ratio during nanoprecipitation process were both elucidated to identify best compromise between size distribution, colloidal stability and high iodine content.

MATERIALS & METHODS

Iodinated homopolymer was formed by radical polymerization of 2-methacryloyloxyethyl 2,3,5-triiodobenzoate monomer with peroxide benzoyl as initiator at 73°C. Nanoprecipitation in presence of PEGylated surfactant was performed to yield intravenously injectable radiopaque suspensions with theoretical iodine content of 15.5, 31 and 62 mg I/mL. Impacts of surfactant-to-polymer weight ratio (30, 40, 50, 60, 70 and 80 wt.%) during the dripping process were studied to find best compromise between suitable size for *in vivo* and iodine content for radio-opacity property. Best formulation was then characterized. Size distribu-

tion and morphology investigations were respectively performed by dynamic light scattering (DLS) and scanning electron microscopy (SEM). *In vitro* study was assayed for iodine quantification by Hexabrix 300® (commercial CA) calibration and to evaluate stability of PNPs by 24h incubation in Fetal Bovine Serum (FBS) and cellular uptake on KB cell line with dye-loaded PNPs (Lumogen Red) by confocal microscopy. *In vivo* X-ray micro-computed tomography (micro-CT) imaging on 3 Swiss mice was run to follow biodistribution after administration over a 100h period.



RESULTS & DISCUSSION

This study was carried out in order to form PNPs suspension containing the highest amount of polymer, and though of iodine element capable of attenuating X-ray, with good stability property in physiological fluid and with a narrow size distribution compatible with *in vivo* application (< 200 nm). Taking in account these required conditions, we succeed to formulate optimal suspension based on spherical PNPs with a mean diameter of 163 nm (PDI 0.09) as shown in Figure 1.

Excellent colloidal stability in FBS of the selected PNPs suspension was notified by an absence of change of size distribution or aggregates formation as checked by visual observation. Among all PNPs suspensions, the optimal one involved the use of 60wt.% of surfactant for a theoretical iodine concentration of 62 mg I/mL. Iodine quantification proved that the selected suspension was 59 mg I/mL which was assumed quite significant and adequate to yield satisfying contrast enhancement. Confocal microscopy investigation revealed that no internalization and none specific interaction occurred between KB cells and dye-loaded PNPs (It should be noted that encapsulation of fluorophore probe within PNPs did not lead to a change of PNPs hydrodynamic diameter indicating that cells were exposed to PNPs with similar design than

ARTICLE

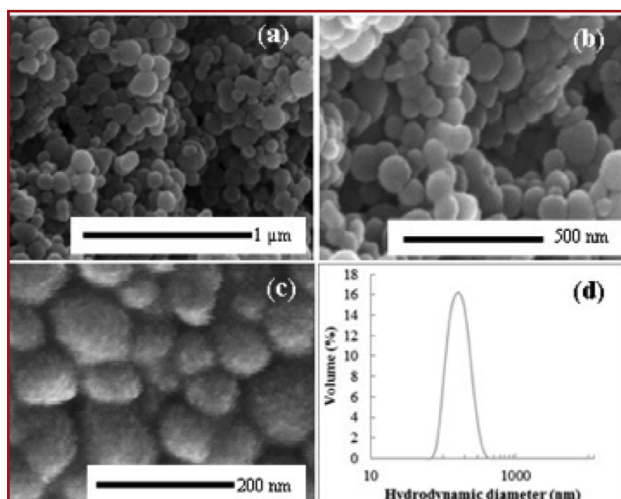


Fig. 1: Electron microscope and DLS investigations on the selected PNPs suspension. (a, b, c) SEM pictures at different magnification. (d) Size distribution profile.

those without dye loading). It means that PNPs would not interfere with biological entities once administrated in mice and exposed to *in vivo* media. Consequently, the biodistribution would only be based on passive targeting due to the stealth and non-functionalized surface of iodine-loaded PNPs.

The *in vivo* assays were all performed with micro-CT for follow-up after intravenous injection in the tail vein of Swiss mice. No adverse side effects were observed on animals over the period of the study. This ensured that a non-toxic PNPs-based CA was formulated. Figure 2 depicts coronal and axial sections of mice at different time after *in vivo* administration. It clearly demonstrated that PNPs were spontaneously and quickly accumulated in liver and spleen 1h after injection. Contrast enhancement was quantified using Hounsfield scale and was respectively 191 HU for spleen and 141 HU for liver. Contrasts remained similar over the whole follow-up period.

The half-lifetime in blood pool was estimated at around 20 min which was relevant regarding the absence of contrast in the heart at 1h post-injection. According to these results, it was assumed that blood clearance might have been done by hepatic and splenic routes. As to the distribution of the injected dose between the two contrasted compart-

ment, it was calculated based on volume of liver and spleen, respectively $4.37 \pm 0.19\%$ $0.48 \pm 0.13\%$ of mice body weight and X-ray attenuation quantification, that the liver received 61% whereas the spleen accumulated 9% of the injected dose. Although the spleen was more contrasted than the liver, the spleen did not contain a higher dose than the liver. Such paradox can be easily explain by the fact that the liver is much bigger than the spleen indicating that it is able to accumulate a higher amount of CA than the spleen. However, due to its smaller volume, the spleen is able to concentrate more the received dose than the liver leading to a best contrast enhancement.

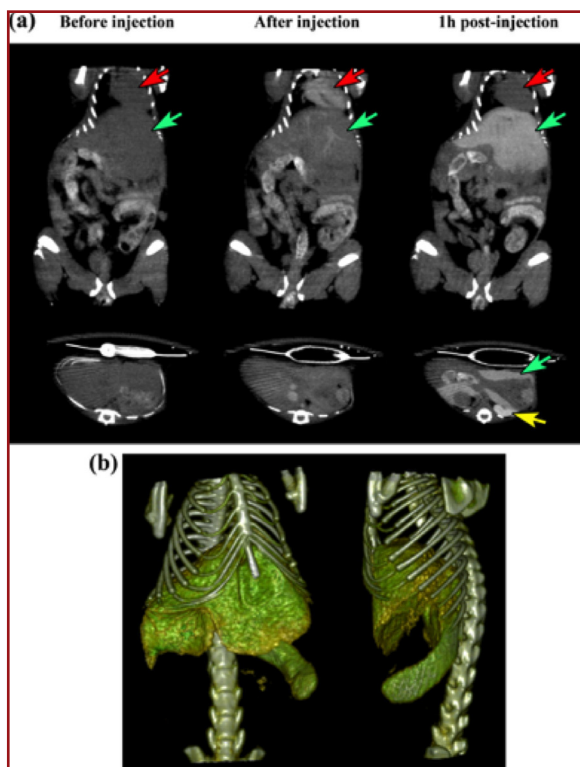


Fig. 2: *In vivo* micro-CT scans (a) before, after and 1h after intravenous injection of the as-prepared CA (a 10% dose of the blood volume). Pictures show coronal and axial sections of mice. Heart, liver and spleen are respectively indicated by red, green and yellow arrows. (b) Liver and spleen 3D volume imaging.

CONCLUSIONS

The achievement of the production of a non-toxic radiopaque PNPs-based CA

was successfully done. It was though proved that nanoprecipitation technique allowed to trap a huge amount of iodine element thanks to its grafting onto polymer backbone involved in the dripping process. The as-nanoprecipitated CA was based on 163 nm spherical PNPs with 59 mg I/mL and 60 wt.% of PEGylated surfactant. Owing to the stealth surface due to PEGylated hairy shell, passive targeting of PNPs occurred and lead to image two soft tissues, the liver and the spleen, via micro-CT with satisfying contrast enhancement. Clear delineation of the liver and the spleen was observed by significant whitening and remained visible over the whole period of study on laboratory animals.

REFERENCES

- Li X., Anton N., Zuber G., Vandamme T. Contrast agents for preclinical targeted X-ray imaging, *Adv. Drug Deliv. Rev.* 2014, 76 (21), 116–133.
- Elsabahy M., Heo G.S., Lim S.-M., Sun G., and Wooley K.L. Polymeric Nanostructures for Imaging and Therapy, *Chem. Rev.* 2015, 115, 10967–11011.
- Fuchs A.V., Gemmell A.C., Thurecht K.J. Utilising polymers to understand diseases: advanced molecular imaging agents, *Polym. Chem.* 2015, 6, 868–880.
- Galperin A, Margel D, Baniel J, Dank G, Biton H, Margel S. Radiopaque iodinated polymeric nanoparticles for X-ray imaging applications, *Biomaterials*, 2007, 28 (30), 4461-4468.
- Fessi C., Devissaguet J-P., Puisieux F., Thies C. Precipitation of film-forming material and biologically active substance from solvent-non-solvent mixture. 1992, US 5118528 A

Acknowledgements

The authors would like to greatly thank Bouquey, M., Collot, M., Weickert, J-L., and Messaddeq, N. from University of Strasbourg and the CERMEP-imagerie du vivant from University of Lyon for their contributions to this work.



Justine Wallyn

Strasbourg University, CAM
Strasbourg, France
justine.wallyn@etu.unistra.fr

ENCAPSULATION OF PANCREATIC ISLET CELLS FOR TYPE 1 DIABETES TREATMENT

Bitar, C., Markwick, K.E., Hoesli, C.A., McGill University, Canada

INTRODUCTION & OBJECTIVES

Type 1 diabetes is a chronic autoimmune disease, involving the attack of the beta cells of the pancreas by the immune system. This causes a decrease in insulin production, and a resulting increase in blood glucose levels in the body. A common treatment involves periodic insulin injections, which leads to glucose variations (Liu, 2015). This poses a risk of long-term complications, in addition to the immediate negative impact on patient quality of life, including pain and bruising.



Islet transplantation has emerged as a clinical option that avoids the need for exogenous insulin in 44% of the patients for at least 3 years (Barton, 2012). The islets are currently obtained from allogeneic donors. To avoid islet rejection, the patients are placed under lifelong immunosuppression, which leads to increased risk of undesirable side effects such as opportunistic infection, hypertension, or cancer. To avoid the need for immune suppression, the islets could be encapsulated in immunoprotective alginate microbeads.

Current nozzle-based encapsulation methods cannot accommodate wide ranges of viscosities of the encapsulation material. Hence, most uncoated alginate beads studied in literature are permeable

to antibodies. Stirred emulsification encapsulation is a scaleable process that solves this issue, however it produces beads with a wide size distribution (Hoesli, 2010). Microchannel emulsification (MCE) is a novel process that could enable the production of monodisperse high-concentration alginate beads, while achieving production rates as high as $1,200 \text{ L h}^{-1} \text{ m}^{-2}$ (Kawakatsu, 1999).

We previously developed a MCE device that can produce uniform alginate beads for islet encapsulation and transplantation. Preliminary process development by modifying parameters such as dispersed and continuous phase flow rates, surfactant type, microchannel dimensions, and material, resulted in the production of beads with diameters ranging from 3 to 5 mm, with a low coefficient of variation of ~5% (Markwick, 2016). Further optimisation of this MCE process is required to achieve a target controlled alginate bead size of approximately 600 μm , which is suitable for islet encapsulation.



Droplet generation in MCE is a spontaneous process driven by interfacial tension, viscous, and inertial forces, requiring little energy input. As shown in Figure 1, the interfacial tension force between the continuous and alginate phase acts against droplet formation, while the buoyancy force due to the density difference between the two phases promotes droplet formation.

As such, the continuous phase fluid selection in the MCE process will play a determining role in droplet formation and size. Two key properties of the continuous phase that will impact droplet formation and size are the interfacial tension and density difference

between the to-be-dispersed and the continuous phase fluids. The objective of this work is to determine the effect of the selected continuous phase on interfacial tension and density difference. The results of this work will provide a design basis to select the most promising continuous phase fluid for MCE production of monodisperse 600 μm diameter beads.

MATERIALS & METHODS

The MCE device (Figure 2) includes two flow chambers placed above and below a hydrophobic polytetrafluoroethylene (PTFE) microchannel plate. The 1-mm thick PTFE plate consists of three oblong rectangular microchannels of approximately 110 μm x 700 μm dimensions. A continuous phase fluid flows through the top chamber, into a collection vessel. The to-be-dispersed 1.5% alginate (FMC Manugel® GHB alginic acid, FMC BioPolymer) phase, autoclaved for 30 minutes, flows into the bottom chamber, and droplets form as the fluid passes upwards through the microchannels. In this configuration, the dispersed phase (alginate) is lighter than the continuous phase. For continuous phase fluids that are lighter than the alginate solution, this configuration was inverted. The continuous phase fluids considered in this study were 3MTM Novec™ 7500 Engineered fluid, light mineral oil (Fisher Scientific), and glyceryl trioleate (~65%, Sigma-Aldrich). Mineral oil was the original fluid used in the stirred emulsification process.

The interfacial tension between the conti-

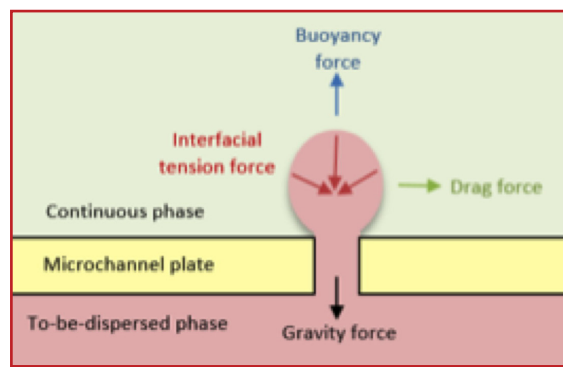


Figure 1. Forces acting in MCE droplet formation, where the density of the continuous phase is greater than that of the to-be-dispersed phase.

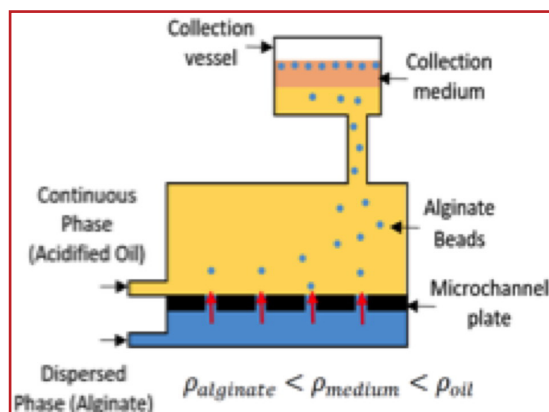


Fig 2. Lab-scale MCE setup for a continuous phase density greater than the to-be-dispersed phase density.

ARTICLE

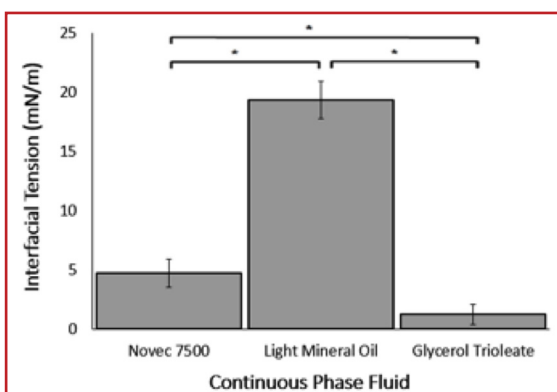


Figure 3. Interfacial tension between alginate phase and continuous phase fluids. The error bars represent the standard deviation of $n=3$ runs. $*p<0.05$

nuous and dispersed phases was measured using a DCAT 11 Dynamic Contact Angle Meter and Tensiometer at the NanoQAM laboratory (Montréal, Québec, Canada), which employs the Wilhelmy Plate method. The fluid densities were determined by dividing the mass by the volume (measured with a 25-mL volumetric cylinder) of each fluid. The statistical analysis used for comparing two samples was a one-way analysis of variance (ANOVA), with p -values less than 0.05 considered statistically significant, followed by Tukey and Scheffe post-hoc tests.

RESULTS & DISCUSSION

Interfacial Tension

Interfacial tension is a primary force affecting droplet formation. The interfacial tension between the continuous and to be dispersed phase fluids should be minimized to facilitate the process. As shown in Figure 3, the interfacial tension between glyceryl trioleate and alginate was significantly lower than the values measured for Novec 7500 or mineral oil. Based on interfacial tension alone, glyceryl trioleate would be the best contender

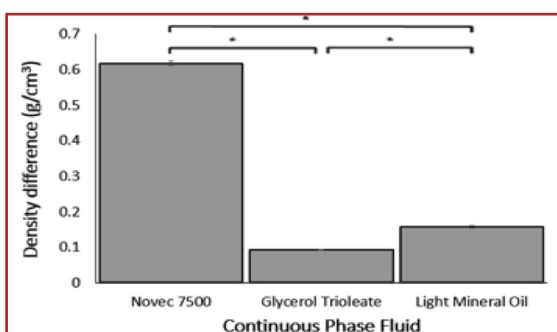


Figure 4. Density difference between alginate phase and continuous phase fluids. The error bars represent standard deviation of $n=3$ runs. $*p<0.05$

for the MCE process, followed by Novec 7500.

Density difference

Figure 4 displays the density difference between various continuous phase fluids and the alginate dispersed phase.

Novec 7500 had a significantly higher density difference with the dispersed phase than the other oils. The mineral oil not only had a high interfacial tension with the alginate phase, but also had a low density difference value. Although glyceryl trioleate showed promise as a continuous phase due to its low interfacial tension with the alginate phase, the density difference was the smallest compared with the other continuous phase fluids.

Overall, Novec 7500 fluid was the most promising continuous phase fluid among the three alternatives tested due to its relatively low interfacial tension and high density difference with the dispersed phase, both of which promote droplet formation. Figure 5 displays toluidine blue-O stained alginate beads produced using Novec 7500 as the continuous phase in the MCE process. The average bead diameter was 2.9 mm, with a coefficient of variation of 9.3%.

CONCLUSIONS & PERSPECTIVES

A MCE device was successfully designed, with the ability to produce uniformly-sized beads with relatively low coefficients of variation. Interfacial tension and density difference measurements confirmed the use of Novec 7500 as a more promising alternative compared to the mineral oil originally tested, or another alternative considered (glyceryl trioleate). Further optimization is required to achieve a bead size suitable for islet encapsulation (~600 μm). Such optimization includes studying the effects of emulsifiers (such as dodecyl alcohol-10-glycol ether), alginate concentration, flow rate, microchannel dimensions, and microchannel plate material on bead size and production rates. These findings will advance diabetes research by providing an alternative process to produce high-concentration monodisperse alginate beads.

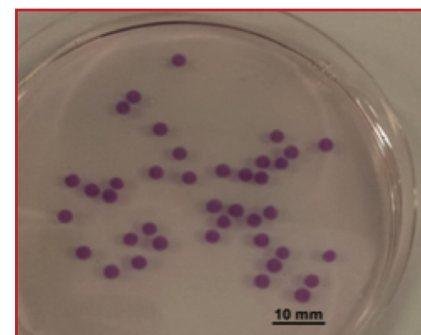


Fig 5. Toluidine blue-O stained alginate beads produced using Novec 7500 as the continuous phase fluid in the MCE system.

The MCE process could also be used to manufacture encapsulated products in the medical, pharmaceutical, food and cosmetic industries.

REFERENCES

- Barton, F.B., Rickels, M.R., Alejandro, R. et al. Improvement in outcomes of clinical islet transplantation: 1999-2000, *Diabetes Care*. 2012, 35 (7) 1436-1445.
- Hoesli, C.A., Raghuram, K., Kiang, R.L.J. et al. Pancreatic cell immobilization in alginate beads produced by emulsion and internal gelation, *Biotechnol. Bioeng.* 2010, 108 (2) 424-434.
- Kawakatsu, T., Komori, H., Nakajima, M. et al. Production of monodispersed oil-in-water emulsion using cross-flow-type silicon microchannel plate, *Journal of Chemical Engineering of Japan*. 1999, 241-244.
- Liu, X., Li, X., Zhang, N. Wen, X. Engineering β -cell islets or islet-like structures for type 1 diabetes treatment, *Med. Hypotheses*. 2015, 85 (1) 82-84.
- Markwick, K.E., Dussault, M.A., Bégin-Drolet, A. and Hoesli, C.A. Microchannel emulsification: a novel approach to cell encapsulation, *Bioencapsulation Research Group*. 2016, 12-13.



Christina Bitar
McGill University
Montreal, PQ, Canada
christina.bitar@mail.mcgill.ca

VERSATILE CELL MICROENCAPSULATION PLATFORM

Crouigneau R., Bottausci F., Gerber S., Szabó L., Benhamou P.Y., Icard B. and Rivera F. – CEA Leti DTBS, France

INTRODUCTION AND OBJECTIVES

Type 1 diabetes affects around 25 million people in the world. Curing this disease is a major challenge for health care. The most common treatment today is insulin injections, several times a day, but it is constraining and does not provide optimal glycaemic control. Transplantation of islets from human donors is a better hope for stable normoglycemia and a reduction in diabetes complications. However, this treatment requires administration of immunosuppressant that lead to many side effects and complications. Islet microencapsulation might be an alternative of immunosuppressive treatment.



Microcapsules properties depend on polymer properties and encapsulation technologies. Regarding the latter, the most commonly used is the air dripping nozzle, that produces microcapsules of 400-1000 μm in diameter, with a size monodispersity that isn't optimal (CV around 15%). We use here the CellencTM microfluidic platform to produce microcapsules down to 150 μm in dia-

meter with a low size dispersion.

Additionally, two types of alginate have been characterized and used to produce microcapsules. The main drawbacks of alginate are its limited mechanical stability, durability and permeability problems (Mahou R., 2010) Macromolecules. In this paper, we compare the commercially available Pronova SLG100 alginate (Novamatrix) with an innovative PEGylated alginate that combines common alginate ionic binding with covalent binding using poly(ethylene-glycol) molecules grafted on the alginate backbone. It has been shown that these covalent bindings increase mechanical stability of the microcapsules (Mahou R., 2010 ; Mahou R., 2015).

We demonstrate that the CellencTM microfluidic platform can be used and adapted for different biopolymers within a large range of viscosity and physico-chemical properties.

MATERIAL AND METHODS

Microfluidic design and fabrication

The alginate microcapsules are produced within the CellencTM microfluidic platform. First, alginate droplets are

generated using a Micro Flow Focusing Device (MFFD) previously described (Le Vot S., 2008) : the alginate flow is sheared by the non-miscible continuous phase (soybean oil), producing a droplet. The droplet is then transferred automatically in a gelling solution, and finally in a physiological serum, thanks to phase transfers modules in the microfluidic cartridge. The size and shape of the capsules are controlled by adapting the channels size, the cartridge design and the pressures used for alginate, oils, gelling solution and physiological serum.

Table 1: Surface tension and contact angles of different alginates in soybean oil

Alginate	Contact angle (°)	Surface tension (mN/m)
LS1/082-4%	126,45 \pm 1,43	11,434 \pm 0,42
SLG100-3%	139,1	16,992 \pm 0,52

The CellencTM microfluidic cartridge is shown in Figure 1. It is a home-made hybrid system made of one silicon chip sealed within a cyclic olefin polymer (COC) cartridges. In the silicon chip, microfluidic channels are dry etched with standard microelectronic technologies to obtain 200 μm large and deep microfluidic channels. The MFFD and phase transfers (Dalle P., 2012) are integrated into the silicon chip. Gelation channels are integrated into the plastic cartridge. Both silicon chip and plastic cartridge are functionalized to obtain hydrophobic channels.

Capsules characterization

Capsules were produced in this microfluidic platform, with commercial alginate (Pronova SLG100-3%, Novamatrix), and innovative PEGylated alginate LS1/082-4% (EPFL). As previously described before, this PEGylated alginate is issued from the commercially available sodium alginate Kelton HV (CP KELCO, $[\eta]=813\text{mL}\cdot\text{g}^{-1}$ in 0,1M NaCl, G/M=0.67), on which Poly Ethylene Glycol (PEG) molecules are grafted on the hydroxyl group, with a 14.3% rate.

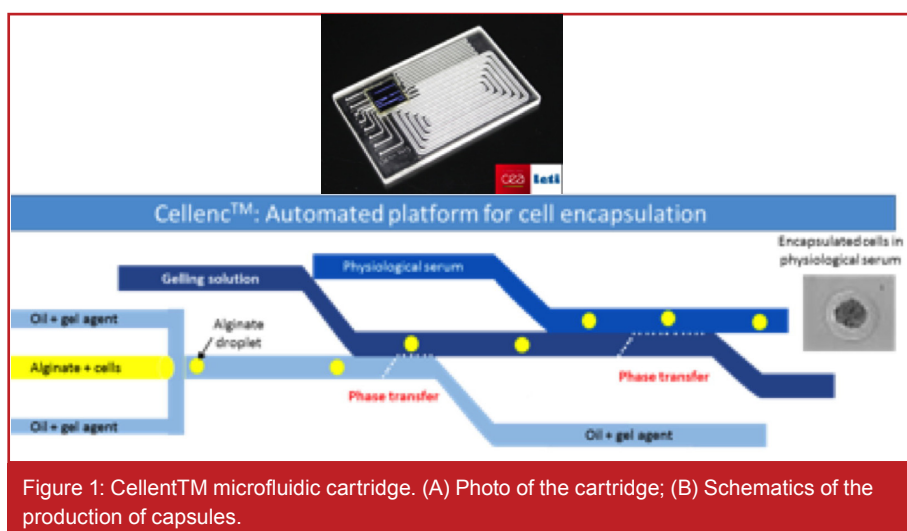


Figure 1: CellencTM microfluidic cartridge. (A) Photo of the cartridge; (B) Schematics of the production of capsules.

ARTICLE

Microcapsules were imaged with phase contrast microscope, and analysis of the size and shape of the capsules were done with the software ImageJ. Aspect Ratio (AR) (ratio between small and large diameters: spherical for 1) was characterized.

Biopolymers characterizations

Rheological properties of both alginates were measured on Malvern Bohlin Gemini rheometer, using a 1/60 cone. Viscosities were obtained either by fitting the rheological measurements with Carrea-Yasuda model (high viscosity), or from the plateau of the rheology curves (low viscosity).

Contact angles of the different alginates were measured using Krüss DSA100, by forming a drop on a silanized silicon surface immersed in Soybean oil.



RESULTS AND DISCUSSION

Rheology

Rheological curves of the two alginates are presented on Figure 2, showing a shear-thinning behavior. Viscosity of SLG100-3% (3.16Pa.s) is around 30 times higher than the one of LS1/082-4% (87.9mPa.s).

Contact angle and surface tension

Contact angle and surface tension impact the production and properties

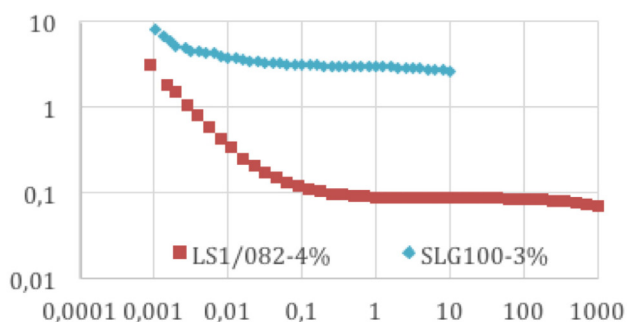


Figure 2 : Viscosity of different alginates (Pa.s) versus shear rate (s⁻¹)

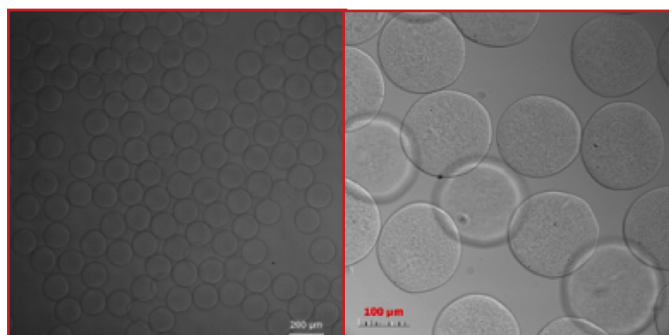


Figure 3 : Capsules obtained in Cellenc™ microfluidic platform. (A) Pronova SLG100-3% capsules; (B) PEGylated Kelton alginate capsules.

of microcapsules. Low contact angle lead to wettability of the polymer to the microchannels and high surface tension to higher shear rate needed to form the capsules. The measurements for both biopolymers are presented on the table below. The silanization makes the surface highly hydrophobic (contact angle > 90°) for both biopolymers. However, LS1/082-4% alginate has lower contact angle than Pronova SLG100-3%, which means that it is more wettable with the surface.

Capsules production and analyse

Considering these characterizations, parameters in the microfluidic platform were adapted to produce capsules.

Microcapsules obtained with the Cellenc™ microfluidic platform are shown in Figure 3. Microcapsules diameter were characterized to be 188,2±2,7µm (CV: 1.5%) for Pronova SLG100-3% and 201±11µm (CV: of 5.5%) for LS1/082-4%. For both polymers, Aspect Ratio was close to 1 (1.054±0.028 for SLG100-3% and 1.06±0.03 for LS1/082-4%).

CONCLUSIONS AND PERSPECTIVES

These results showed the ability of the Cellenc™ microfluidic platform to produce automatically microcapsules from different biopolymers. Low size dispersion (CV:5%) microcapsules have been produced independently

from their physico-chemical properties and for a large range of viscosity.

Currently, capsules production with the innovative PEGylated alginate in the microfluidic platform are carried on, to eventually encapsulate insulin secreting cells first, and pig islets then. Encapsulated cells and islets

will be tested in vitro and in vivo. The good control in size and shape of the capsules should give better results in terms of cells survival and biocompatibility, and the better mechanical resistance of PEGylated alginate should give long term mechanical stability and durability of the capsules.

REFERENCES

- Mahou R., Wandrey C., *Macromolecules*, 2010, 43, 1371-1378
- Mahou R., Borcard F., Crivelli V. et al., *Chem. Mater.*, 2015, 27, 4380-4389.
- Le Vot S. et al., *Proceedings of the XVI International Conference on Bioencapsulation*, 2008
- Dalle P. et al., 2012, *Technical proceedings of the 2012 NSTI Nanotechnology conference and expo*

Acknowledgements

This work has been funded by the French National Agency (ANR-15-CE18-0022).



Roxane Crouigneau
CEA
DRT-LETI-DTBS-LBCP
Grenoble, France
roxane.crouigneau@cea.fr

USE OF A KENICS STATIC MIXER FOR CONTINUOUS MICROENCAPSULATION

Goibert, S. R.L.^a - Segers, M.^a - Teixeira, R.^b - Kuhn, S.^c - Braeken, L.^{a,c} - Thomassen L. C. J.^{a,c}

INTRODUCTION & OBJECTIVES

The development of microcapsules is mainly performed in lab-scale batch equipment. Scaling these batch reactors is difficult due to mass and heat transfer limitations and requires several steps between lab scale (g/h) and production scale (100 kg/h). On the contrary, flow reactors show improved mass and heat transfer properties compared to batch reactors and are therefore more scalable, keeping heat and mass transfer properties constant without the need for re-optimization on a large scale.¹

KATHOLIEKE UNIVERSITEIT
LEUVEN

For microencapsulation, with capsules containing a liquid core, emulsion based encapsulation techniques, include coacervation, in-situ polymerization and interfacial polycondensation.² The emulsions required for these encapsulation processes can be generated in flow a number of devices and are ranked according to throughput as follows flow focusing (FF) (106 part./s), < microchannel emulsification (MCE) and membrane emulsification (ME) (10-100 L/(m² h) < static mixer (SM) (1000 L/h) < active mixer (AM) (100-20,000L/h). However when compared on monodispersity of the droplets generated, the lowest relative spread (covariance (CoV)) is obtained in FF, < 3 %, followed by MCE < 5% and ME 10-20%. Static mixers show a CoV > 20% and active mixers >30%.^{3,4} Static mixers are studied and compared using liquid-liquid systems, of which the emulsion is seldom used for microencapsulation.

Furthermore, the spread of the droplet size distribution is often not shown, and the Sauter mean diameter is reported, rather than the actual mean diameter. The flow devices mentioned provide only the emulsification step of a two-step process. The second step, entails the shell formation reaction and requires heat and time. In flow chemistry this is performed in a residence time reactor, i.e. a reactor channel, with or without additional mixing structures.

The objective of this research is to ascertain the potential of static mixers for emulsion based microencapsulation in a fully continuous reactor setup. In the current study the emulsion template for a microencapsulation process, based on interfacial polycondensation, is generated in a recirculation loop. The static mixers investigated is a Kenics static mixer (KSM) and the curing step is performed in a coiled tubular reactor. The novel aspect of the current setup is the fact that the emulsion is not created semi-batch wise, instead both phases of the emulsion are pumped continuously into the recirculation loop where first contact of the phases occurs. The input and exit flow rates are identical.

MATERIALS & METHODS

Microencapsulation

The microencapsulation method used is based on an oil-in-water interfacial polycondensation, forming a polyuria shell.⁵ The continuous phase is a 13 wt.% arabic gum solution (AG) (Sigma-Aldrich, Saint Louis, Missouri, US). The dispersed phase contains hexyl acetate (HA) (Sigma-Aldrich, Saint Louis, Missouri, US) combined with Suprasec® 2030 (Devan Chemicals, Ronse, Belgium). Continuous and dispersed phases are combined in a volume ratio of 10:4 to generate the emulsion. The polymerisation initiator, 2,4,6-triaminopyrimidine (TAP) (Sigma-Aldrich, Saint Louis, Missouri, US), is prepared in ultrapure water, and is added to the emulsion in a volume ratio of 4.8 : 10.



Emulsification and curing in flow

The recirculation loop setup is shown in Fig. 1 A. A Kenics static mixer (KSM) (Metrohm Belgium n.v., Antwerp, Belgium) with an internal diameter of 6.8 mm is placed inside and the liquid is pumped through with a peristaltic pump (Verder Ltd, Castleford, UK). The effects of superficial velocity (0.06, 0.16 and 0.27 m/s) and the number of static mixers elements (1, 4, or 13) are studied. The continuous feed flow rate is 15 ml/min and enters the loop through a T-piece. The oil and water phase are pumped separately through a Y-pre-mixer using peristaltic pumps (Watson-Marlow Fluid Technology Group, Falmouth, UK). The coarse emulsion (droplets of 2 – 4 mm in diameter) enters the loop via a T-mixer located directly in front of the static mixer. At the exit (Y-mixer connection) the generated emulsion is combined with the TAP solution in a Y-mixer, resulting in a total flow rate of 22.2 ml/min. The Y- and T-mixers are supplied by Reichelt Chemietechnik GmbH + Co., Heidelberg, Germany. 80 ml of the exit stream is collected in an EasyMax 102 batch reactor system (Mettler-Toledo, LLC, Columbus, US) for curing. The reaction mixture is heated from 22 to 65°C at 3.4°C/min. Upon reaction completion the mixture is cooled rapidly in an ice bath. The full continuous setup combines part A and B of Fig. 1. The tubular reactor is made out of PTFE with an internal diameter of 4 mm (Polyfluor Plastics bv, Breda, Netherlands). The tubular reactor is dimensioned to obtain a residence time of 10 minutes and is placed in a water bath at 65°C. The continuous exit stream is quenched directly in ice cold water.

Characterisation of Microcapsules

The Capsule size distribution (CSD) is determined with optical imaging. Microscopic images are made with an Axiocam 105 color (Carl Zeiss, Oberkochen, Germany) and analysed using ImageJ. The mean capsule diameter (d_{mean}) and the

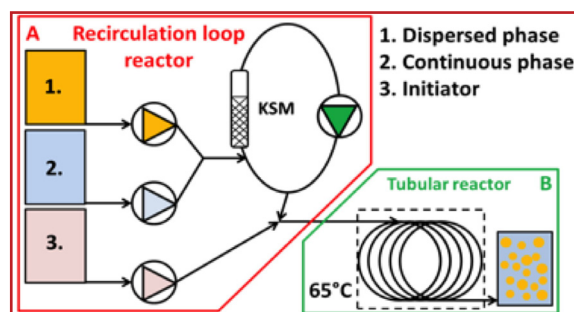


Fig. 1: Schematic representation of flow reactor setup for microencapsulation.

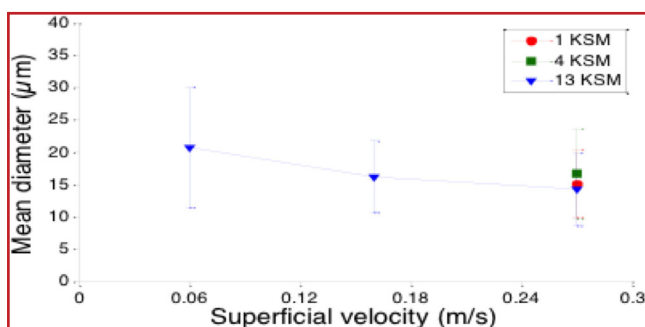


Fig. 2: Influence of superficial velocity and the number of KSM on the mean capsule diameter, error bars indicate the spread of the capsule size distribution.

covariance ($CoV = \sigma/d_{mean}$), with σ the standard deviation) indicating the relative spread of the distribution are quantified for each particle size distribution.

RESULTS & DISCUSSION

Fig. 2 shows the influence of superficial velocity on the mean capsule diameter and spread of the particle size distribution. Error bars indicate the spread of the distribution curve. For a 13 element KSM, a 2.6 increase in superficial velocity (0.06 to 0.16 m/s) results in a decrease in mean diameter from 20.8 to 16.2 μm . The standard deviation also decreases, resulting in a drop in covariance from 45% to 34%. A further increase (1.7 fold) in velocity to 0.27 m/s does not change the mean capsule diameter or the covariance of the distribution. At this high superficial velocity, the number of static mixers elements is decreased to 1 and 4. This reduction of the number of element does not influence the spread or the mean capsule diameter which remained in the region of 15 μm . With a recirculation loop, the fluid entering the loop, passes multiple times through the static mixer. This ensures steady state conditions, i.e. equilibrium of droplet breakup and coalescence, is reached. For the current experiments the number passes through a single mixing element ranges from 39 (for one static mixer at 0.06 m/s) to 503 (13 static mixers at 0.27 m/s). To shift the equilibrium toward smaller droplets and possibly a lower spread, even higher superficial velocities are needed.

The condition with the lowest spread (13 KSM's at recirculation rate of 0.16 m/s) is used to generate the emulsion for continuous curing. A throughput of 195 g (capsules)/h is obtained. After curing in flow

the capsule size distribution shows a slight increase in increase in mean capsule diameter (17.1 μm versus 15.2 μm , in flow and batch respectively). The covariance has increased from 33.2% to 41.8%; see Fig. 3

A possible cause of this coalescence of droplets is the flow behaviour. The batch reactor shows a Reynolds number of 3663,

for the continuous phase, which indicates the liquid is well mixed in the transition zone between laminar ($Re < 10$) and turbulent ($Re > 10,000$) mixing. The Reynolds number inside the flow reactor is 80, indicating laminar flow (turbulence occurs at $Re > 2100$ in pipe flow). This flow type is characterised by a parabolic velocity profile. Droplets at the tube wall move slowly while droplet in the centre move at a maximum velocity, this could induce collisions leading to larger droplets through coalescence. To avoid droplet coalescence ideal plug flow, characterised by radial mixing and no axial mixing, is needed.

CONCLUSIONS AND PERSPECTIVES

A fully continuous setup for the microencapsulation of ethyl acetate with a polyurea shell is developed. A throughput of 195 g (capsules)/h is realised. The emulsification is performed in a recirculation loop reactor enabling high number of passes through the static mixer element. A KSM showed a mean droplet diameter of 16.2 μm with a $CoV = 34.1\%$, at 0.16 m/s, with 13 mixing elements. An increase in superficial velocity decreased the mean diameter and the spread, however above a superficial velocity of 0.16 m/s

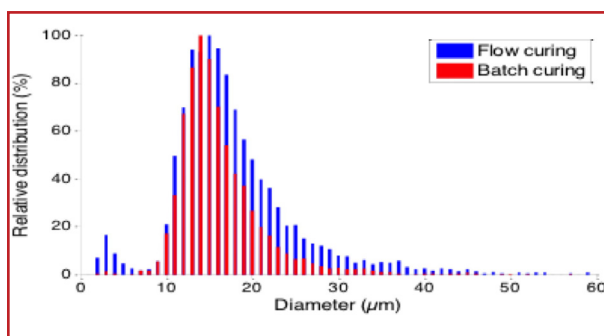


Fig. 3: Size distribution of batch and flow cured capsules generated in a recirculation loop (13 KSM at 0.16 m/s).

the capsule size distribution showed little change. The number of static mixer elements did not influence the capsule size distribution at high flow rates (0.27 m/s). This is attributed to the large number of recirculations in the loop reactor leading to steady state conditions. Curing in flow increases the spread of the capsule size distribution, compared to batch curing, mainly due to coalescence of droplets. Further research will focus on characterization of the flow behaviour and temperature profile inside the reactor to clarify the mechanism of coalescence. The range of experimental conditions will be increased to gain a better insight in the controllability of capsule size through the superficial velocity. Additional parameters will be the static mixer type and the feed flow rate. To test flexibility of the recirculation loop, other chemical encapsulation processes will be tested in the setup.

REFERENCES

- (1) Wiles, C.; Watts, P. *European J. Org. Chem.* 2008, No. 10, 1655–1671.
- (2) Jyothi, N. V. N.; Prasanna, P. M.; Sakarkar, S. N.; Prabha, K. S.; et al. *Microencapsul.* 2010, 27 (3), 187–197.
- (3) Martin-Banderas, L.; Ganan-Calvo, a. M.; Fernandez-Arevalo, M. *Lett. Drug Des. Discov.* 2010, 7 (4), 300–309.
- (4) Vladislavljević, G. T.; Kobayashi, I.; Nakajima, M. *Microfluid. Nanofluidics* 2012, 13 (1), 151–178.
- (5) Nguyen, L. T.; Hillewaere, X. K. D.; Teixeira, R. F. A.; van den Berg, O.; et al. *Polym. Chem.* 2015, 6 (7), 1159–1170.

Full addresses

^a KU Leuven, Faculty of Industrial Engineering, Lab4U; Agoralaan building B box 8, 3590 Diepenbeek Belgium

^b Devan Chemicals, Klein Frankrijkstraat 6, 9600 Ronse, Belgium.

^c KU Leuven, Chemical Engineering, Celestijnenlaan 200F, 3001 Leuven Belgium



AROMA ENCAPSULATION FOR ANTIBACTERIAL AND ECO-FRIENDLY TEXTILE FINISHING

Sharkawy, A.¹, Fernandes, I.², Barreiro, F.², Rodrigues, A.³, Shoeib, T.^{1, 1} The American University in Cairo, Egypt

INTRODUCTION AND OBJECTIVES

Encapsulation imparts new properties and added value to conventional fabrics (Nelson, 2002). Most of the commercially available microcapsules for textile applications are made of melamine-formaldehyde, urea-formaldehyde or phenol-formaldehyde resins, which have significant negative health and environmental effects. Recently, there has been a growing interest in the replacement of these resins with safe and environmentally benign materials.



The process of fixing the microcapsules onto textile substrates is critical in ensuring their durability and effectiveness. The commonly known industrial methods used for this involve the use of two main groups of binders; polymeric resins, and polyfunctional crosslinking agents. Polymeric resins are reported to partially inhibit the release of fragrance from the microcapsules. The chemical cross-linkers are subdivided into formaldehyde based, e.g., formaldehyde and glutaraldehyde, and non-formaldehyde based, such as polycarboxylic acids.

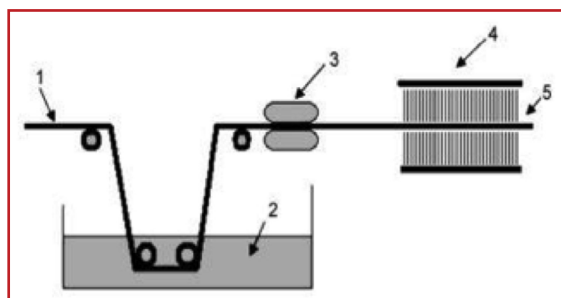


Figure 1: Fixation steps of the microcapsules onto cotton fabrics. Scheme adapted from (Rodrigues, 2009). 1. Untreated fabric 2. Impregnation bath 50 °C (contains microcapsules, citric acid and catalyst) 3. Foulard (0.1 MPa) 4. Thermofixation (drying at 90°C and curing at 150°C) 5. Treated fabric

This work aimed at conferring fragrant and antibacterial properties to cotton fabrics employing new methodologies utilizing non-toxic and environmentally friendly materials.

MATERIALS AND METHODS

Microcapsules were prepared by the complex coacervation method (Butstraen, 2014) but with some modifications. D-Limonene was used as the core material. Size distribution and mean particle size were determined by laser diffraction. Encapsulation efficiencies were measured by GC-FID. Fixation of the microcapsules onto fabrics was accomplished by using citric acid as a non-toxic cross-linker (See Figure 1). The fixation of the microcapsules onto fabrics was examined using FTIR-ATR. The percent of bacterial inhibition of the impregnated cotton fabrics and of the control fabric samples was assessed by the Standard Test Method under Dynamic Contact Conditions (ASTM Standard E 2149-01); with a modification that involved the renewal of the bacterial inoculum after each washing cycle.

RESULTS AND DISCUSSION

The produced microcapsules showed 94% encapsulation efficiency and a mean diameter of 39 μm . The particle size distribution is shown in Figure 2.

SEM was used to examine the cotton fabrics impregnated with microcapsules (Figure 3). Impregnated fabrics were also examined by SEM after being washed with 2% commercial soap followed by 0.1N acetic acid and deionized water to investigate the effect of washing on the adhesion of the microcapsules to the fabrics. The process was

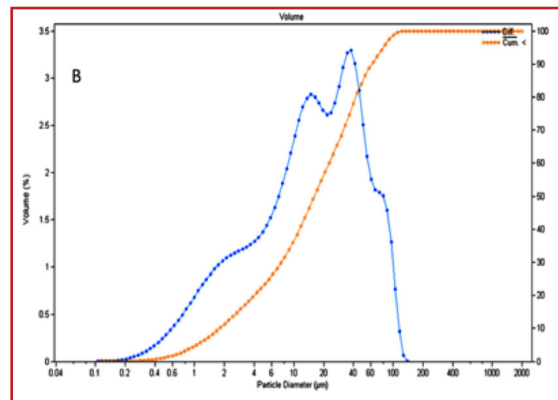


Figure 2: The particle size distribution in volume of the produced limonene microcapsules.

repeated three times. SEM images showed the microcapsules being still attached to the fabric (Figure 4).

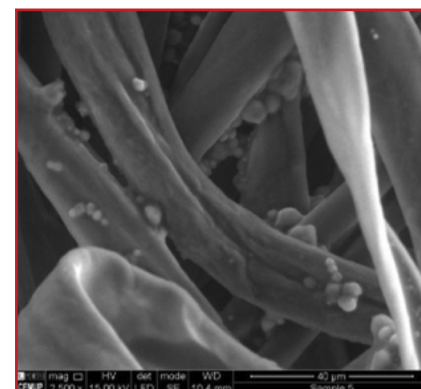


Figure 3: SEM image of cotton fabric impregnated with limonene microcapsules.

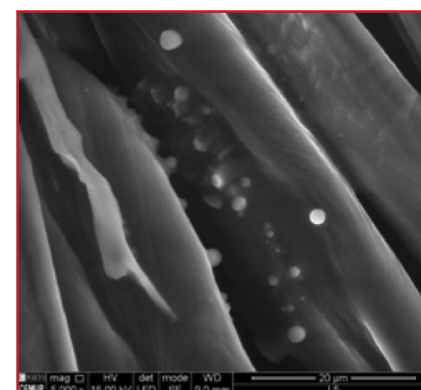


Figure 4: SEM image of impregnated cotton fabric after washing for three cycles.

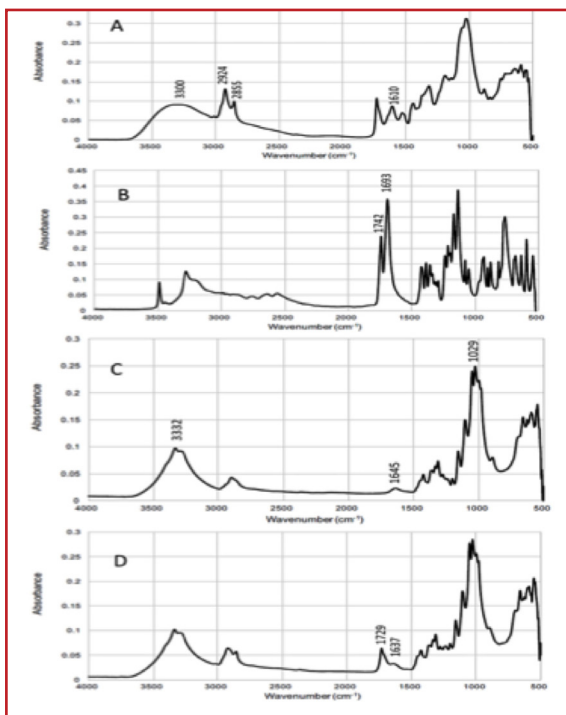


Figure 5: FTIR spectra of A) microcapsules B) citric acid C) control fabric D) treated fabric

The peak at 2855 cm^{-1} in the FTIR spectrum of the microcapsules (Figure 5) indicates the successful complex coacervation between chitosan and gum Arabic, as reported in the literature (Butstraen, 2014). The spectrum of cotton fabric impregnated with limonene microcapsules did not show the presence of the sharp peaks at 1742 cm^{-1} and 1693 cm^{-1} characteristic of citric acid, which is compatible with its effective bonding with the $-\text{OH}$ groups of the cotton cellulose. The spectrum of

the grafted cotton fabric also revealed the appearance of a new peak corresponding to the $\text{C}=\text{O}$ ester stretching at 1729 cm^{-1} , which was absent in the control cotton fabric sample confirming the covalent attachment between the polymeric shell of the microcapsules with cotton cellulose via citric acid reaction.

Bacterial inhibition tests were conducted against *E. coli* and were calculated according to the following formula:

where B is the CFU/ml for the treated fabric sample after the specified contact time and A is the CFU/ml for the inoculum before the addition of the treated fabric. The results of the assays are shown in Figure 6. The impregnated fabric showed 95.9% bacterial reduction after 15 minutes of dynamic contact. Every 15 minutes

the fabric sample was washed with sterilized water and placed in contact with a new bacterial inoculum in order to take samples for colony counting. The percent bacterial reduction decreased with time, it was maintained throughout the 8 renewal cycles with values higher than 25% reduction.

CONCLUSIONS AND PERSPECTIVES

Imparting a durable antimicrobial finish to cotton fabrics by using microcapsules was successfully achieved using green and non-toxic materials. Future work will focus on maintaining the aroma durability of the treated fabrics according to end-use application (e.g., washing and abrasion test cycles).

REFERENCES

- Nelson G. Application of microencapsulation in textiles. *Int. J. Pharm.* 242, 55-62 (2002).
- Butstraen C., Salaün F. Preparation of microcapsules by complex coacervation of gum Arabic and chitosan, *Carbohydr. Polym.*

99, 608-616 (2014).

- Rodrigues S. N., Martins I. M., Fernandes I. P. et al. Scentfashion®: Microencapsulated perfumes for textile application, *Chem. Eng. J.* 149, 463-472 (2009).



Acknowledgements

This work was funded by the American University in Cairo.

It was also in part financed by the project POCI-01-0145-FEDER-006984 – Associated Laboratory LSRE-LCM funded by FEDER funds through COMPETE2020 – Programa Operacional Competitividade e Internacionalização (POCI) and by national funds through Fundação para a Ciência e a Tecnologia (FCT) in Portugal.

Full addresses

¹ Department of Chemistry, The American University in Cairo, New Cairo 11835, Egypt

² LSRE-LCM, Polytechnic Institute of Bragança, 5300-253 Bragança, Portugal

³ LSRE-LCM, Faculty of Engineering, University of Porto, Porto 4200-465, Portugal

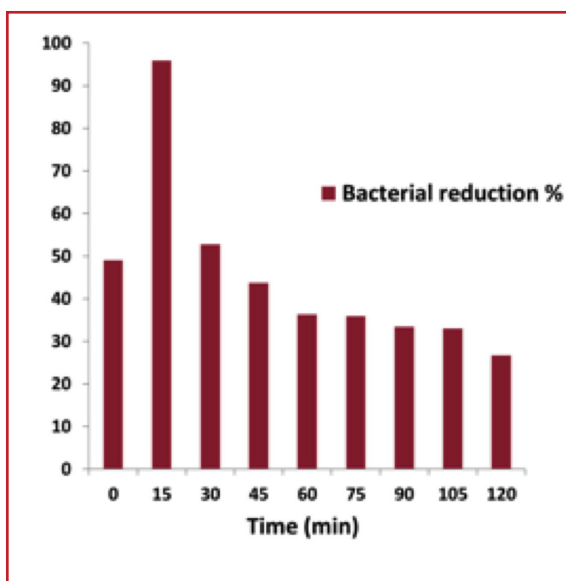


Figure 6: Results of the bacterial reduction % of cotton fabric impregnated with limonene microcapsules.



Asma Sharkawy

The American University in Cairo
Department of Chemistry
New Cairo, Egypt
asmaa_s@aucegypt.edu

ENGINEERING PEGYLATED ALGINATE HYDROGELS FOR CELL MICROENCAPSULATION

Noverraz, F., Szabó L., Passemard, S., Wandrey, C., Gerber-Lemaire, S. – EPFL, Switzerland

INTRODUCTION

The progress of medical therapies, which rely on the transplantation of microencapsulated cells, depends on the quality of the encapsulating material. Such material has to be biocompatible, its physical characteristics have to be adjustable, and the microencapsulation process must be simple and not harm the cells (Figure 1). In this context development and investigation of hydrogels, which meet all the requirements for cell transplantation, are main subjects of interest.

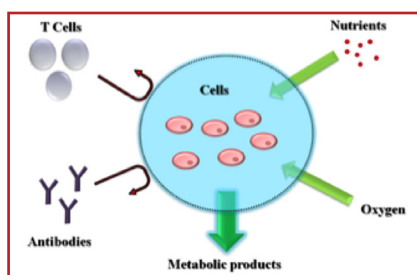


Fig 1: Optimal microsphere properties.

MATERIALS AND METHODS

Hydrogels presented herein are composed of covalently and electrostatically crosslinked combinations of sodium alginate (Na-alg), poly(ethylene glycol) derivatives (PEG), and functionalized Na-alg which favourably mimic the natural environment of cells.

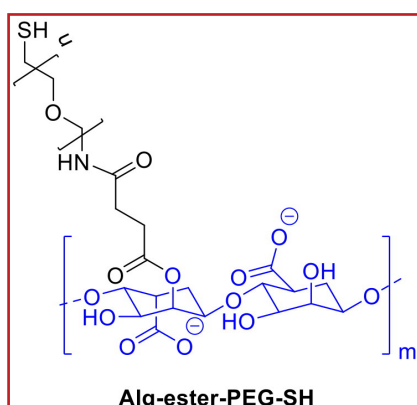


Fig 2: Structure of PEGylated alginate.

In this approach, PEGylated hydrogel microspheres were produced by combining the ionotropic gelation of Na-alg using calcium ions with covalent cross-linking of thiol end groups grafted onto Na-alg (Figure 2 & 3).

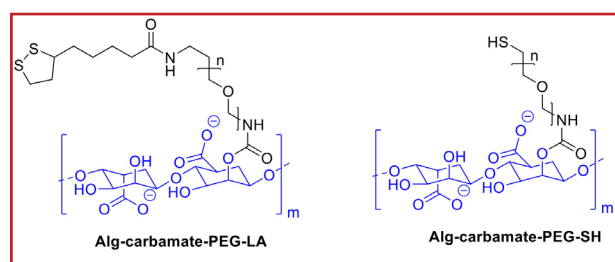


Figure 3: Structure of PEGylated alginate with carbamate.

The synthesis of PEGylated alginates started with Na-alg High Viscosity (HV). In order to preserve the ionotropic gelation ability of the alginate, carboxylate functional groups of the starting material were remained untouched. Only the hydroxyl groups were modified with either succinic anhydride to introduce a carboxylic acid terminal groups for further functionalization or with carbodiimidazole to activate this position for direct post-modification. Next, the coupling with heterobifunctional PEG derivatives containing amine, thiol or lipoyl end functionalities was performed.

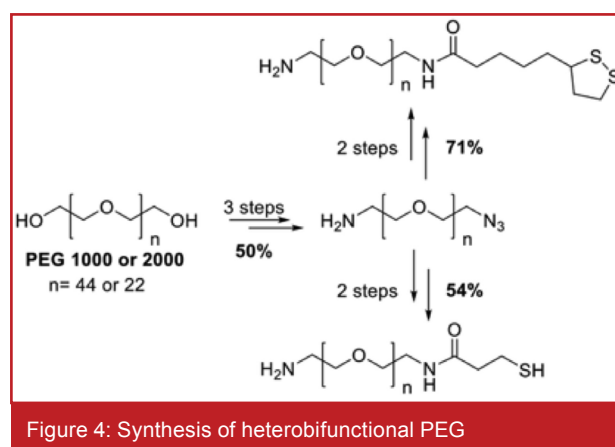


Figure 4: Synthesis of heterobifunctional PEG

In parallel, the possibility to synthesize a variety of heterobifunctional PEG derivatives starting from homobifunctional PEG 1000 or 2000 was explored. The synthesis implied a desymmetri-

zation step from a mono-Staudinger reduction, following a protocol previously established in our laboratory (3. Passemard, 2013). The coupling with protected 2-mercapto-propionic acid followed by catalytic reduction of azide functionality, or the coupling with lipoic acid followed by reduction of the azide yielded the desired heterobifunctional PEG derivatives (Figure 4).

A defined concentration of PEGylated alginates in 3-(N-morpholino)propanesulfonic acid (MOPS) solution was then dropped in a gelation bath containing CaCl₂. The microspheres were prepared under sterile conditions employing a coaxial airflow droplet generator (Encapsulator B-395 Pro, Büchi Labortechnik AG), and evaluated for their physical properties (mechanical resistance and elasticity).



RESULTS AND DISCUSSION

The fast ionotropic gelation ensures the spherical shape of the microspheres. Simultaneously, controlled but slowly occurring covalent cross-linking reinforces the hydrogel network and adjusts its permeability.

We present herein the results concerning functionalized alginates with carbamate grafting moiety and PEG 1000 derivatives as they provided the best performance in terms of mechanical properties and durability in physiological environment. Two hydrogels prepared with different

ARTICLE

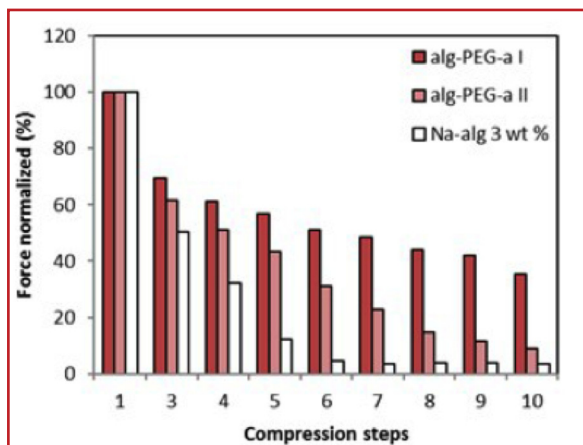


Figure 5: Resistance to 10 successive compressions to 90% of Alg-PEG-SH MS (3 wt %), Alg-PEG-L.A MS (3 wt %) and Ca-alg MS (3 wt %).

PEGylated alginate (Alg-PEG-SH and Alg-PEG-LA) allowed formation of microspheres (MS) (average diameters of 934 ± 101 and 667 ± 98 μm) which were assessed for their mechanical properties under single and repetitive compressions. When compressed to 90% of their initial volume, Alg-PEG-SH MS demonstrated higher mechanical resistance than pure Ca-alg MS, while the values remained in the same range for Alg-PEG-LA MS and pure Ca-alg MS. The shape recovery of the microspheres varies also a lot with respect to their constitutions. The performance of the MS was significantly better for PEG-grafted alginates than for pure Na-alg (Figure 5).

Starting from a 3 wt % solution of polymer, Alg-PEG-SH MS demonstrated almost 40 % shape recovery after 10 compressions while Ca-alg MS showed a complete loss of shape recovery after 4 compressions.

Cell microencapsulation

Both Alg-PEG derivatives were investigated for cell encapsulation using mouse insulinoma cell line MIN6 as model cells. The cells were successfully encapsulated in microspheres presenting a diameter between 500 and 600 μm . The cell viability, assessed by FDA/PI staining at 3 and 15 days after encapsulation reached almost 80 % with both polymers and was stable over time. MS from Alg-PEG-LA appeared degraded over time and out-diffusion of cells was identified from day 10. MS from Alg-

PEG-SH kept their integrity for 15 days. These results indicate the possibility to modulate the stability of microspheres by the chemical composition of the grafted alginates. Free non-encapsulated MIN6 cells and microencapsulated MIN6 cells were subjected to a glucose-stimulated insulin release assay under static conditions, for both MS at day 3 and day 10 after microencapsulation (Figure 6). Stimulation was done at a glucose concentration of 16.7 mM, and the fold increase of insulin release was calculated/expressed with respect to the insulin release at basal glucose concentration of 2.8 mM, which was set as 1. The assay outcome was the same for free MIN6 cells and microencapsulated MIN6 cells, using either Alg-PEG-SH or Alg-PEG-L.A. MS, showing that the insulin-secreting capacity is maintained upon microencapsulation.

CONCLUSIONS

The synthesis of Na-alg derivatives grafted with PEG of different chain length containing thiol and 1,2-dithiolane end groups is presented together with the physical properties of series of microspheres (1. Mahou, 2013) and the feasibility of cell microencapsulation (2. Mahou, 2014; 4. Mahou 2015).

Our approach combines the ionotropic gelation of alginate carboxylate groups and the covalent crosslinking of thiol groups derived from the grafted PEG within the same polymer. The aim is to enhance the robustness of micro-

capsules, which physical properties allow their potential application for xenotransplantation. Further improvement of the polymer is in progress, including variation of the PEG structure and conjugation to bioactive molecules to increase the biocompatibility of the materials by preventing inflammation and fibrosis.

The type of functionality inserted into the PEG chain for the covalent cross-linking influences the stability of the resulting microspheres. Therefore, the functionalization of the alginate derivative can be selected according to certain applications.



REFERENCE

1. R. Mahou, et al. (2013) Combined electrostatic and covalent polymer networks for cell microencapsulation. *Macromol. Symp.* 329(1) 49-57.
2. R. Mahou, et al. (2014) Alginate-poly(ethylene glycol) hybrid microspheres for primary cell microencapsulation. *Materials* 7(1) 275-286.
3. Passemar, et al. (2013) Convenient synthesis of heterobifunctional poly(ethylene glycol) suitable for the functionalization of iron oxide nanoparticles for biomedical applications. *Bioorg. Med. Chem. Lett.* 23(17) 5006-5010.
4. Mahou, R. et al. (2015) Tuning the Properties of Hydrogel Microspheres by Adding Chemical Cross-linking Functionality to Sodium Alginate. *Chem. Mater.* 27, 4380–4389 (2015)

Acknowledgements

Montanari, E., Gonelle-Gispert, C., Bühler, L. – HUG, Switzerland.



François Noverraz
EPFL, Lausanne, Switzerland
francois.noverraz@epfl.ch

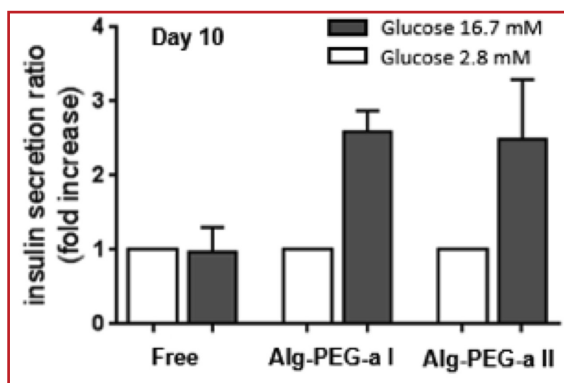


Figure 6: Glucose-stimulated insulin release for non-encapsulated MIN6 cells (Free) and MIN6 cells microencapsulated in MS of Alg-PEG-SH and Alg-PEG-LA.

DEVELOPMENT OF PAROMOMYCIN MICROPARTICLES FOR CUTANEOUS LEISHMANIASIS TREATMENT

Matos, A.P.S.^{1,2}; Azevedo, J.R.¹; Viçosa, A.L.³; Ricci-Junior, E.⁴; Holandino, C.²; Ré, M.I.¹

INTRODUCTION AND OBJECTIVES

Leishmaniasis belongs of the group of neglected infectious diseases caused by protozoan parasites of the genus *Leishmania* (Tiuman, 2011; Singh, 2012) and is one of the major health problems in the world. The current treatment for cutaneous leishmaniasis (CL) has many side effects (toxic drugs), low patient adhesion (long treatment with injectable formulations) and parasites resistance. These factors are motivating the development of new pharmaceutical formulations, as micro or nanoparticles. One of the drugs used in CL treatment is paromomycin (PM), an aminoglycoside antibiotic used intravenously and topically with poor oral absorption (Tiuman, 2011). There are few studies approaching the physicochemical characterization of PM and development of new formulations of this drug. PLGA [poly (lactic-co-glycolic acid)] is the most important polymer investigated in microparticles development due its biodegradability and bioavailability (Ansary, 2014). The aim of this work is to develop PLGA microparticles containing PM by spray drying

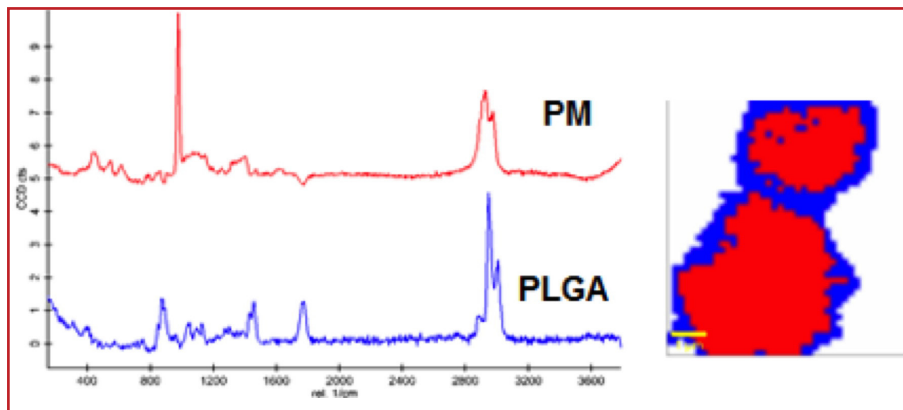


Figure 2 – RAMAN spectra of spray dried PM-PLGA particles (S2).

for controlled release and intralesional administration for CL treatment. Two different methods of association of PLGA with PM were tested: 1. from an organic solution containing dispersed drug and dissolved polymer using a two fluid nozzle (single droplets); 2. from two separate solutions containing dissolved drug and polymer (core-shell droplets) using three fluid nozzle.

MATERIAL AND METHODS

Paromomycin microparticles were prepared using a spray dryer B-290 (Büchi, Switzerland) with an inert loop B-295. Acetone was used as solvent. Two types of nozzle were used: (S1 - two fluid nozzle and S2 - three fluid nozzle). The inlet temperature was set to $60^{\circ}\text{C} \pm 1^{\circ}\text{C}$ and the outlet temperature was kept at $43^{\circ}\text{C} \pm 3^{\circ}\text{C}$. Heated nitrogen gas was used as drying/carrying gas with flow rate of 500L/h.

The microparticles were characterized by

scanning electron microscopy (Philips XL30 ESEM-FEG, Philips), differential scanning calorimetry (Q200, TA Instruments), AFM-RAMAN Spectroscopy (Witec Alpha 300AR, Witec) and infrared spectroscopy (Thermo Nicolet is10, Thermo Scientific).



RESULTS AND DISCUSSION

All formulations were developed for 30% (w/w) of PM load (dry mass). Figure 1 exhibits a schematic representation of the nozzles related to the expected solid structures and those obtained from experiments as shown by SEM analysis. In both cases the resultant spray dried microparticles are spherical. When microparticles were formed from an organic solution containing PM dispersed into an acetone PLGA solution (S1), PM microparticles seem be partly recovered by small particles of PLGA (Fig. 1b). However, spray-dried microparticles obtained from core (aqueous solution of PM) and shell (acetone PLGA solution) droplets (S2) revealed a similar core-shell structure (Fig. 1c). This kind of core-shell structure was also confirmed by RAMAN analysis shown in Figure 2.

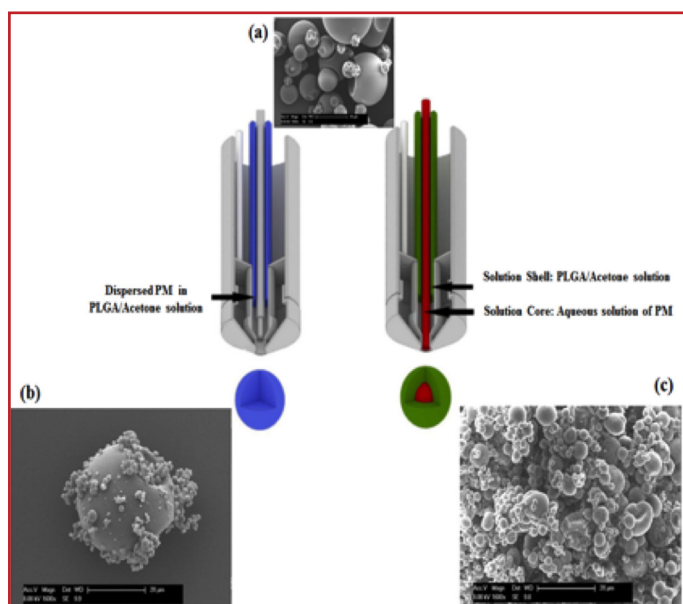


Figure 1 – SEM images of (a) unprocessed PM microparticles; spray dried PM-PLGA microparticles: (b) S1, (c) S2. (Note: Scheme adapted from Kaspar, 2013).

Table 1: Thermal analysis of DSC

Samples	1st Heating cycle		2nd Heating cycle	
	Tg °C	ΔCp J/g.°C	Tg °C	ΔCp J/g.°C
PM	-	-	-	-
PLGA	40.80	0.4726	42.24	0.5390
S1	39.79	0.4974	41.33	0.4533
S2	41.06	0.2356	42.90	0.2670

Table 1 shows the results from DSC analysis in two heating cycles. PM alone did not present characteristic thermal properties (Tg or Tf). Both spray-dried products presented only a glass transition temperature (Tg) around 40°C, close to that of PLGA polymer, with no significant difference between them.

In other to investigate possible interactions between PM and PLGA, FTIR analysis were performed (Figure 3).

The PLGA spectrum showed peaks at 2997cm⁻¹ and 2917cm⁻¹ (CH₂ stretch), 1750cm⁻¹ (C=O stretch), 1380cm⁻¹ (CH₂-CH wagging vibration) and at 1180cm⁻¹ and 1098cm⁻¹ (C=O ester group). The PM spectrum showed characteristic peaks at 3408cm⁻¹ (NH₂ amine group), at 1632cm⁻¹ (N-H ben-

ding coupled with C-N stretch), at 1534cm⁻¹ (CH₂ bending) and at 1027cm⁻¹ (C-O-C stretch). Some characteristic peaks of both PM and PLGA can be seen in the PM-PLGA physical mixture. S1 spray dried PM-PLGA microparticles presented peaks at 3380cm⁻¹ (NH₂ amine group), 1080 cm⁻¹ (C-O-C stretch) corresponding to PM peaks and at 2990cm⁻¹, 2940cm⁻¹ (CH₂ stretch), 1750cm⁻¹ (C=O stretch) corresponding to PLGA peaks (b in Figure 2). By its turn, S2 presented similar spectrum when compare to S1 differing only in peaks intensity at 2990cm⁻¹ and 2940cm⁻¹ (CH₂ stretch, corresponding to PLGA peaks) (a in Figure 2). These data suggest no molecular interactions between drug and polymer.



IMT Mines Albi-Carmaux
École Mines-Télécom

CONCLUSIONS & PERSPECTIVES

Two different manners for associating PM and PLGA were investigated here. In both case, no molecular interactions were detected between the components. However, S1 and S2 microparticles presented different physical structures. S2 microparticles could be more interesting to promote controlled release. This study is on-going to optimize S2 formulation looking for PM controlled release. Further, the leishmanicidal activity of these formulations will be evaluated.

REFERENCES

- Ansary R.H., Awang M.B., Rahman M.M. Biodegradable poly(D,L-lactic-co-glycolic acid) based micro/nanoparticles for sustained release of protein drugs – A

review. Trop J Pharm Res. 2014, 13 (7), 1179-1190.

- Kaspar O., Tokarova V., Nyanhongo G.S., Gubitz G., Stepanek F. Effect of cross-linking method on the activity of spray-dried chitosan microparticles with immobilized laccase. Food Bioprod Process 2013, 91 (4), 525-533.
- Singh N., Kumar M., Singh R.K. Leishmaniasis: Current status of available drugs and new potential drug targets. Asian Pac J Trop Med 2012, 5 (6), 485-497.
- Tiunan T.S., Santos A.O., Ueda-Nakamura T., Filho B.P.D., Nakamura C.V. Recent advances in leishmaniasis treatment. Int J Infect. Dis. 2011, 15, e525-e532.

Acknowledgement

We thank Fundação de Amparo à Pesquisa do Rio de Janeiro (FAPERJ) for Ana Paula Matos's PhD scholarship, GALA® technological platform and S. Delconchetto, P. Accart, C. Roland and L. Haurie from Rapsodee Research Center for technical support.

Full Addresses

1 Rapsodee Research Center, Ecole des Mines d'Albi Carmaux, France. anapaulasmatos@gmail.com

2 Universidade Federal do Rio de Janeiro - UFRJ, Brazil.

3 Laboratório de Farmacotécnica Experimental, Instituto de Tecnologia em Fármacos, FIOCRUZ, Brazil.

4 Laboratorio de Desenvolvimento Galênico, Universidade Federal do Rio de Janeiro - UFRJ, Brazil.

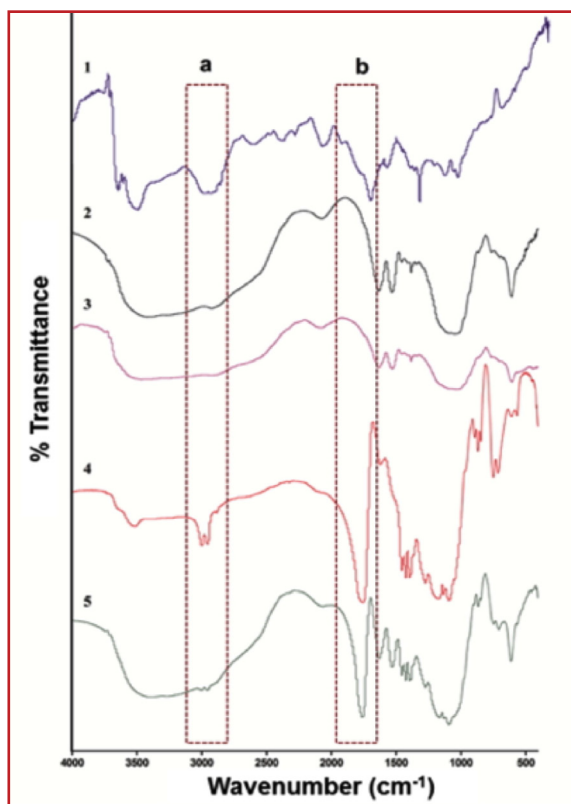


Figure 3 – IR spectra of (1) free PLGA, (2) free PM, (3) PM-PLGA physical mixture, (4) PM-PLGA microparticles S1 and (5) PM-PLGA microparticles S2.



Ana Paula Dos Santos Matos
Mines Albi-Carmaux
Centre Rapsodee
Albi, France
anapaulasmatos@gmail.com

EVALUATION OF DRUG LOADING IN AMORPHOUS SOLID DISPERSION FOR EFAVIRENZ DELIVERY

Costa, B.L.A., Sescousse, R., Sauceau, M., Ré, M.I.- Rapsodee Center, France

INTRODUCTION AND OBJECTIVE

Poorly water-soluble drugs have steadily grown on the global pharmaceutical industry. The technological approach focused on rendering the drug amorphous in nature to improve apparent solubility, dissolution rate and bioavailability remains a challenge since amorphous state is metastable in nature with a potential to undergo recrystallization (Wlodarski, 2015). In order to prevent this conversion, amorphous materials have been stabilized as solid dispersions using generally polymeric materials for stabilization (Lu, 2016).



An amorphous solid dispersion (ASD) is basically a drug-polymer two-component system in which the mechanism of drug dispersion is the key to understanding its behavior. Such formulations impart an antiplasticizing effect on the amorphous compound yielding an increase in the glass transition temperature thereby reducing molecular mobility (Patel, 2013). However, in order to achieve adequate stabilization, solid dispersions are often produced with a relatively low drug load (<30% w/w) where the drug is dispersed in the polymer at the molecu-

lar level. The problem is that a low drug loaded ASD requires a large dose to ensure therapeutic efficacy.

The insertion of high drug load formulations on the market is expected to meet patients demand for fixed, unique and smaller dosage combinations products. Furthermore, the supersaturated combinations may reduce dosage amounts as well as decrease the production in the pharmaceutical industries to supply cost savings. The aim of the current work was to verify the possibility to formulate high drug loaded (>40%) ASD of Efavirenz (EFV) by spray drying. EFV is a non-nucleoside reverse transcriptase inhibitor used in the first-line treatment of HIV and a class 2 drug in the Biopharmaceutical Classification Systems (BCS) with low solubility (3-9 µg/mL) and high permeability (Hoffmeister, 2016). To stabilize the amorphous drug, an amphiphilic and water-soluble copolymer named Soluplus® was used.



MATERIALS AND METHODS

EFV was kindly supplied by Cristalia Ltd (Itapira, Brazil), Soluplus® (polyvinyl caprolactam-polyvinyl acetate-polyethylene glycol) was obtained from BASF corporation (Ludwigshafen, Germany) and Ethanol was used as organic solvent (Carlo Erba, Italy).

A Buchi B-290 minispray dryer (Buchi Labortechnik AG, Flawil, Switzerland) equipped with Inert Loop B-295 and an integrated two-fluid 0.7 mm nozzle was used to produce the ASD samples. Compressed nitrogen was used as the drying/carrying gas with a flow rate of 600 L/h. The so-

lution feed rate was typically 3g/min, the inlet temperature was set to 80 +/- 2°C and the outlet temperature was maintained at 59°C +/- 2°C. The feeding solution was prepared by dissolving EFV in a 10 (w/w) % solution of Soluplus in ethanol. Binary mixtures EFV-Soluplus containing 40wt%, 60wt% and 85wt% of EFV were formulated as spray-dried powders.

X-ray diffraction (XRD), modulated differential scanning calorimetry (mDSC), Raman spectroscopy scanning electron microscopy (SEM) and dynamic vapor sorption (DVS) were used to characterize the solid state of the spray-dried samples.

RESULTS AND DISCUSSION

Firstly, the absence of Bragg peaks in X-ray diffractograms (Figure 1) of all spray-dried solids indicates the complete loss of the crystalline structure of EFV, which became amorphous during the spray-drying process.

mDSC thermal analysis was performed to investigate the apparent EFV-Soluplus® miscibility. Figure 2 shows the single experimental glass transition temperature (T_g) identified for each binary mixture EFV-Soluplus loaded with 40% to 85%(w/w) EFV, probably corresponding to the formation of an amorphous solid dispersions of EFV-Soluplus. The individual constituents (drug and polymer) were also spray-dried from ethanol solutions and used for comparison

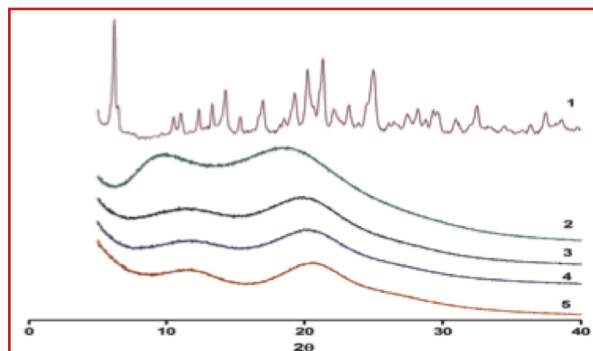


Fig1. PXRD diffractograms of: (1) pure EFV; (2) pure Soluplus®; (3) ASD 40%EFV-Soluplus (w/w); (4) ASD 60%EFV-Soluplus (w/w) and (5) ASD 85%EFV-Soluplus (w/w)

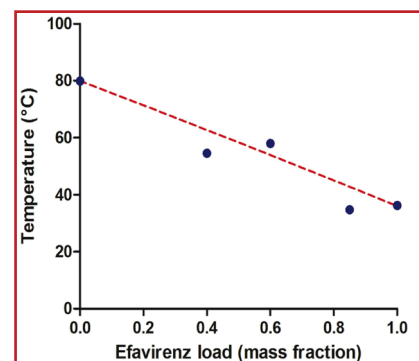


Fig 2. Glass temperature transition (T_g) determined by mDSC (blue circles) and theoretical values by GT equation (dotted red line)

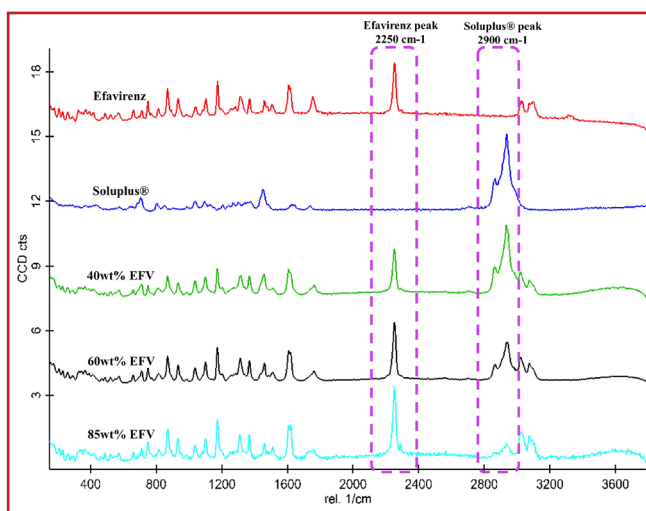


Figure 3. Raman spectra for the ASD EFV-Soluplus with different drug loads: 40%; 60%; 85% (w/w) EFV

purposes (T_g also in Figure 2). The T_g of mixtures are placed as an intermediary between the pure drug and polymer values and are close to the theoretical values of T_g calculated by Gordon-Taylor (GT) equation, which relates the individual contributions of each component in an ideal mixture (with no interactions between the components).

Raman microscopy was also performed for the three ASD EFV-Soluplus (Figure 3). They were evaluated by observing the characteristic peaks of pure drug (peak at 2250 cm^{-1}) and pure polymer (peak at 2900 cm^{-1}). As expected, the increase of the drug load in the mixture (85% > 60% > 40% w/w EFV) corresponded to a more intense characteristic EFV peak. The presence of characteristic peaks of pure components in all ADS Raman spectra confirmed the good mixing between EFV and Soluplus® for all studied drug loads.

Figure 4 presented SEM images of the spray-dried powders. The predominantly spherical particles constituting the ASD

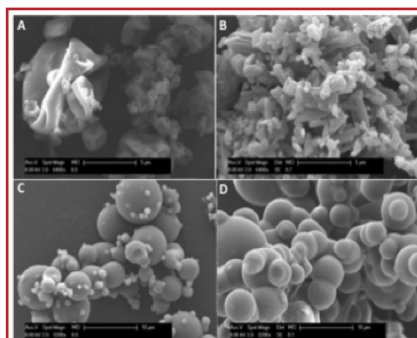


Fig 4: SEM images of (A) spray-dried Soluplus®; (B) unprocessed Efavirenz crystals; (C) 60% (w/w) EFV; (D) 85% (w/w) EFV

EFV-Soluplus are different of the unprocessed EFV crystals that are long rods with regular and organized multi-face geometry (Figure 4.B).

In a complementary study, water sorption isotherms were determined gravimetrically using an automated water sorption analyzer (DVS-2). The samples were subjected to 0–95% relative humidity (RH) sorption-desorption cycle, over 10% RH increments. Figure 5 displays the dynamic vapor sorption (DVS) isotherm plots for the studied samples, showing the percentage change in mass as a function of chan-

ging relative humidity. The reversibility of the water uptake was clearly seen in all cases. Taking as example the curves at 75%RH (Figure 5B) the tendency of increasing the hydrophobic character of ASD EFV-Soluplus by increasing the EFV loading is demonstrated. The decreased affinity to water with increased drug loading could be an interesting attribute for the amorphous phase physical stability.

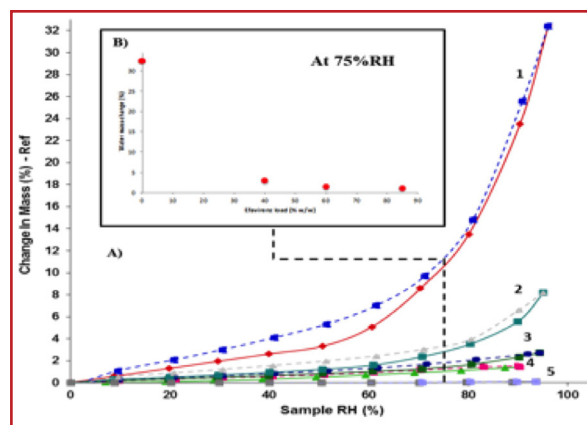


Fig 5. A) DVS isotherms for 1- pure Soluplus®; 2- 40% (w/w) EFV; 3- 60% (w/w) EFV; 4- 85% (w/w) EFV; 5- pure EFV. B) Water mass change (%) at 75%RH for the solid dispersions.

ging relative humidity. The reversibility of the water uptake was clearly seen in all cases. Taking as example the curves at 75%RH (Figure 5B) the tendency of increasing the hydrophobic character of ASD EFV-Soluplus by increasing the EFV loading is demonstrated. The decreased affinity to water with increased drug loading could be an interesting attribute for the amorphous phase physical stability.

CONCLUSION & PERSPECTIVES

A robust formulation with optimal drug load and excipients is one of the key factors of successfully developing an ASD system. In this work, amorphous solid

dispersions of the poorly water soluble compound Efavirenz were prepared at significantly higher drug loadings (40 to 85% EFV w/w) using Soluplus as polymeric carrier and spray drying as the production process. At the best of our knowledge, it is the first study reporting such levels of drug loading in amorphous solid dispersions of EFV. Solubility and dissolution studies are currently being performed and stability studies are on going under stress conditions (40°C, 75%RH and compression tests).

REFERENCES

- Wlrodaski K., Sawicki W., Kozyra A. et al. 'Physical stability of solid dispersions with respect to thermodynamic solubility of tadalafil in PVP-VA' *Eur J Pharm Bio.* 2015, 96, 237-246.
- Lu Z., Yang Y., Covington R. et al. 'Supersaturated controlled release matrix using amorphous dispersions of glipezide', *Int J Pharm.* 2016, 511, 957-968.
- Patel B.B., Patel J.K., Chakraborty S., Shukla D., 'Revealing facts behind spray dried solid dispersions technology used for solubility enhancement', *Saudi Pharm J.* 2015, 23, 352-365.
- Hoffmeister C. R. D., Fandaruff C., Costa M.A., et al. Efavirenz dissolution enhancement III: Colloid milling, pharmacokinetics and electronic tongue evaluation', *Eur J Pharm Sci.* 2017, 99, 310-317.

Acknowledgements

The authors are grateful to Gala® platform (France) for technical support, Cristalia (Brazil) for providing Efavirenz and to S. Delconchetto, V.Nallet, S. Patry, C. Rolland and L. Haurie from Rapsodee Center for respectively DSC, DRX, DVS, SEM and Raman analysis.



Bhianca Lins de Azevedo Costa
Mines Albi-Carmaux
Centre Rapsodee
Albi, France
bhiancalins@gmail.com

SPHEROIDS VERSUS ISOLATED CELLS ENCAPSULATION FOR BIOARTIFICIAL LIVER

Pasqua M., Pereira U., Fleury M.J., Dermigny Q., Legallais C., UTC UMR CNRS 7338, France

INTRODUCTION & OBJECTIVES

Acute liver failure (ALF) is a life-threatening critical illness with an incidence of fewer than 10 cases per million persons per year in the developed world. The growing gap between the number of patients on waiting lists, and the number of donor organs available, has highlighted the need for alternative therapies as a bridge to transplantation or liver regeneration. Two types of extracorporeal liver support systems are nowadays available: artificial and bioartificial liver (BAL). If artificial liver supports are designed to replace the detoxification liver functions, BALs based on tissue engineering, are expected to fulfill the majority of liver functions (Carpentier et al., 2009). The key component of a bioartificial liver is the bioreactor, the cell-housing component. Its role is to keep hepatic cells working physiologically for prolonged period of time. In this scenario, hepatic cell microencapsulation in alginate beads has been recognized as an interesting alternative to classical cell immobilization in hollow fiber membranes. The mechanical properties still need to be tuned to offer the best microenvironment to cells. The biomass (cellular component) is the main pitfall of this promising treatment. Although primary human hepatocytes are still considered the gold standard, their limited availability, as well as logistical issues, hampers their use in BAL. In this context, hepatocyte-like cells (HepaRG, iPS) need to be considered as an alternative. However, the challenge is to induce/maintain the hepatic functions over time. Recently, some authors successfully extended hepatic functions cultivating cells as spheroids before encapsulation (Tostoes et al., 2012). This strategy appears a better way than the use of isolate cells. However, the majority of these studies are focused on toxicology approaches and they do not consi-

der logistic obstacles or costs due to additional manipulation. Therefore, in this study, we propose to compare the biological response of either isolated HepaRG or spheroids encapsulated in alginate beads, to choose the best process for further use in fluidized bed BAL.



MATERIAL & METHODS

Alginate microbeads formation

Alginate Manucol LKX (FMC Biopolymer, Brussels, Belgium) was solubilized in extrusion media (NaCl 154 mM and HEPES 10 mM, pH 7.4) for 24 hours at concentrations of 1%(w/v) and 1.3%(w/v). Microbeads preparation was achieved using the extrusion method adapted in our laboratory (Gautier et al., 2011). Briefly, the solutions were extruded through a 24 G nozzle with a coaxial air flow. The droplets fell into their respective gelation solution bath (NaCl 154 mM, HEPES 10 mM and CaCl₂ 115 mM, pH 7.4) and were allowed to gelify for 15 min at room temperature. Then the beads were washed twice with 710 HepaRG media.

Compression study

The beads were subjected to a classical compression assay following the method previously described by David et al. The beads are compressed at constant speed using a computer controlled device fitted with a 2 N force transducer (machine BOSE Electroforce 3230). Briefly, a single bead was placed on a platform submerged in extrusion solution and compressed until hydrogel failure while

its shape was continuously monitored by a CCD camera. The force exerted by the piston was recorded by the transducer. The compression experiment was analyzed by means of Hertz theory. For each condition, compression tests were performed on 10 bead samples and the Young's modulus was calculated.

Cell culture (amplification)

HepaRG from Biopredict (Rennes, France) cells were routinely propagated in static conditions following the indications reported by the supplier. Cells were passaged every 2 weeks until passage 19, with medium (Biopredict 710 proliferation media) replenishment twice per week. After that, cells were detached and used in different conditions (figure 1).

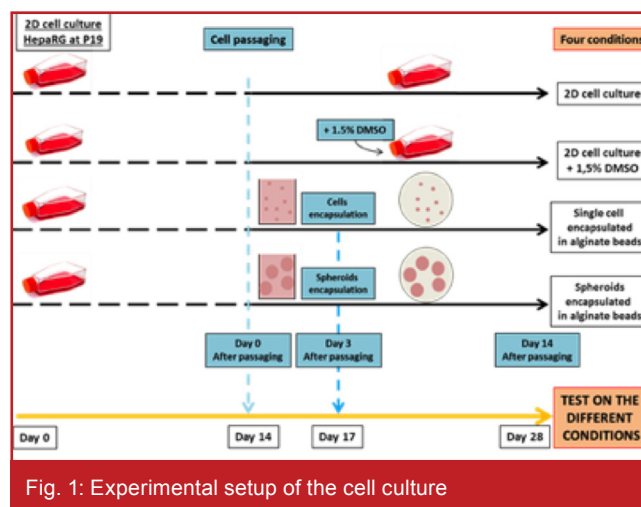


Fig. 1: Experimental setup of the cell culture

2D static culture

HepaRG cells were maintained in conventional 2D culture for 14 days with 710 proliferation media

2D differentiation

HepaRG cells were differentiated in 2D culture for 14 days with 720 differentiation media (following the indications reported by Biopredict International)

Cells encapsulated

HepaRG cells were directly encapsulated as aforementioned at density of 5 millions



ARTICLE

of cells by mL alginate, and maintained until 14 days in proliferation media

Spheroid encapsulated

Cells were suspended in 710 Biopredic proliferation media and inoculated at a density of 3×10^6 cells/dish into glass petri dishes ($\varnothing \times h = 60 \times 12$ mm) coated with Sigmacote® (Sigma-Aldrich). Cells were subject to continuous orbital agitation at 100 rpm with oscillation amplitude of 16 mm (SSL1 orbital shaker, Stuart) in a humidified environment at 37°C and 5% CO₂. After 3 days of aggregation, spheroids were encapsulated with the same process and density, as previously described. After encapsulation, beads are maintained until 14 days in 710 media

Viability and metabolic assay

Viability was assessed by propidium iodide and Hoechst staining. The secretion of albumin was measured by an enzyme-linked immunosorbent assay (ELISA) (human/ rat antibody, Bethyl laboratories, Euromedex). The urea synthesis was quantified by colorimetric urea kit (QuantiChrom Urea Assay Kit, BioAssay Systems). The results were expressed as $\mu\text{g}/\text{days}/10^6$ cells. Xenobiotics function were also measured by EROD assay (phase I) UGT assay (Phase II) and indocyanine green assay (Phase 0 and III).

RESULTS & DISCUSSION

2D HepaRG static culture

HepaRG cells have the ability to develop, during cell culture, from epithelial phenotype to a dual phenotype containing both hepatocyte- and biliary-like cells at confluence (figure 2A). Hepatocyte-like cells seeded at low density reverts to a more undifferentiated phenotype and biliary cells, after removal of hepatocytes, also give rise to both cell populations. The HepaRG cells are thus considered to be progenitor cells.

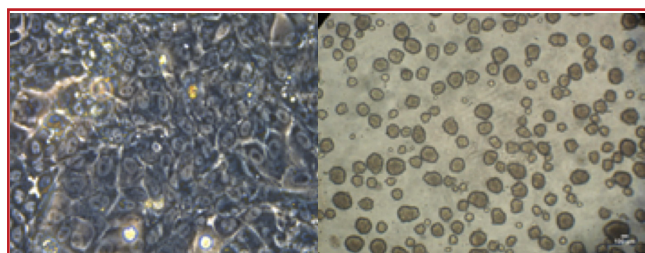


Fig. 2: HepaRG at day 14 (A, 14 days after seeding) and spheroids at 4 days of cell culture (B)

Alginate microbeads at different concentration

The aim was to obtain beads with a mean diameter of 900 μm and a standard deviation within the 5% of the mean value, by means of the encapsulation device developed in our laboratory. The beads diameter depends on different factors such as the coaxial air flow, the distance between nozzle and gelation solution bath, stirring speed and gelation time. After different trials, we were able to set the device in order to obtain beads with a diameter of 900 μm .

Mechanical properties characterization

We performed compression tests on alginate microbeads and for 1%(w/v) their Young's modulus was closer to the physiological one than 1.5%(w/v) (concentration currently used in our laboratory).

Spheroids formation and encapsulation

Three days after continuous stirring in petri dishes, spheroids compact enough to be encapsulated were obtained (figure 2B). The technique, which was first applied to a hepatoma human cell line (C3A) (Figaro et al., 2015) was then successfully applied to HepaRG.

CONCLUSIONS & PERSPECTIVES

Some preliminary tests have been carried out but still a lot of work is in progress, regarding compilation data of the viability and metabolic assay. The aim of this work is the microencapsulation of HepaRG cells into alginate microbeads either as single cells or spheroids, in order to understand which is the best condition, in terms of cell viability and functionality, over time. The evaluation of the impact of alginate matrix stiffness on encapsulated cells and spheroids and also the influence of cells or spheroids on the mechanical properties of the alginate beads will be deeply studied. After this investigation, we will be able to understand which is the best solution for bioartificial liver purposes and in vitro characterization of encapsulate cells or spheroids, in a prototype of bioreac-

tor, will be explored and the behaviour of cells evaluated. Finally, the goal will be the development of a bioartificial liver for small size animal: ALF will be induced in the animal model and the efficacy of the BAL will be evaluated in terms of animal survival over time.

REFERENCES

- Carpentier B., Gautier A., Legallais C. Artificial and bioartificial liver devices: present and future. *Gut*. 58,1690-1702 (2009).
- Gautier A., Carpentier B., Dufresne M., et al. Impact of alginate type and bead diameter on mass transfers and the metabolic activities of encapsulated C3A cells in bioartificial liver applications. *Eur. Cells & Materials* 21, 94-106 (2011).
- Figaro S., Pereira U., Rada H., et al. Development and validation of a bioartificial liver device with fluidized bed bioreactors hosting alginate-encapsulated hepatocyte spheroids. *Conf. Proc. IEEE Eng. Med. Biol. Soc.*,1335-1338 (2015).
- Tostões R.M., Leite S.B., Serra M. et al. Human liver cell spheroids in extended perfusion bioreactor culture for repeated-dose drug testing. *Hepatology* 55, 1227-1236 (2012).
- David B., Barbe I., Barthès-Biesel D., Legallais C., Mechanical properties of alginate beads hosting hepatocytes in a fluidized bed bioreactor. *Int. J. Artif. Organs*. 29(8):756-63 (2006)

Acknowledgement

The project is funded by PIA-RHU ILite (ANR16-RHUS-0005)

Full address

Université de Technologie de Compiègne, UMR CNRS 7338 Biomechanics and Bioengineering, Compiègne, France.



Mattia Pasqua
UTC
UMR CNRS 7338
Compiègne, France
mattia.pasqua@utc.fr

IMMOBILIZATION OF PROBIOTIC BACTERIA IN BIOPOLYMER MATRIX TO INCREASE GASTROINTESTINAL SURVIVAL

Chanut, J., Leonard, L., Watt, M., Husson, F., Saurel, R., - Agrosup Dijon, France

INTRODUCTION AND OBJECTIVES

Lactococcus lactis Elafin (Elafin pSec plasmid) is a probiotic lactic acid bacterium (LAB) with recognized benefits on human health (Kechaou et al., 2013).

The present study aimed to entrap probiotic LAB in a sodium alginate/sodium caseinate aqueous two-phase gel system to stabilize and maintain their viability, to protect them against the harsh gastro-intestinal environment, and to provide a controlled release in the colon (Léonard, 2015).

Sodium alginate/sodium caseinate (Alg-Cas) is a thermodynamically incompatible aqueous two-phase system because both polymers were similarly negatively charged at neutral pH giving an emulsion-like structure.

It can be possible to cross-link one phase by gelation i.e. the continuous one and use this matrix to encapsulate active compounds like probiotic (Léonard, 2016).



Two encapsulation systems were tested. On one hand gels were obtained by using the natural acidifying properties of LAB to liberate calcium ions progressively from calcium carbonate (CaCO_3), which caused the gelation of the co-existing phases. On a second hand, beads were formed by an extrusion/dripping method with the use of an electrostatic force to pull droplets of alginate/caseinate solution into a CaCl_2 bath.

Survival of bacteria was monitored during *in vitro* static gastric and intestinal digestions for three conditions: gel, beads and cell suspension.

Besides, confocal microscopy was used to study the localization of the bacteria in the biopolymeric gel.

MATERIALS AND METHODS

Bacterial strain, media and growth conditions.

Lactococcus Lactis Elafin was pre cultured using the procedure described by Léonard (2015).

Preparation of polymeric stock dispersions and encapsulation systems

A 4% (w/w) dispersion of sodium alginate (Alg) (Fisher Scientific, Loughborough, United Kingdom) and a 10% (w/w) dispersion of sodium caseinate (Cas) (Acros Organic, Geel, Belgium) were prepared in sterile distilled water in a sterile flask, stirred overnight at room temperature, and then stored at 4 °C. The caseinate dispersion was heat-treated for 10 min at 90°C before use.

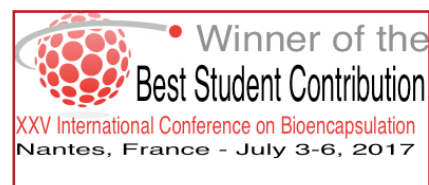
Before experiments, probiotic bacteria cells had been recovered by centrifugation from a LAB culture. The cells were then washed twice in Tryptone Salt Broth (TSB) at 5000g, 15 min, and 4°C. After the last centrifugation, the cells were re-suspended in 5% (w/w) glucose solution.

Gel production: Alg-Cas solutions (1.5% (w/w)—4% (w/w)) were reconstituted from the stock dispersions. Calcium carbonate powder was then poured at 20 mmol.L^{-1} and mixtures were stirred vigorously. Lastly, probiotic LAB in the 5% (w/w) glucose solution was added at 20% (w/w) to the Alg-Cas mixture. Samples were conditioned in syringe and then incubated 6 h at 30 °C for gelation.

Beads production: the same Alg-Cas solutions were reconstituted from the stock dispersions. Then probiotic LAB in the glucose solution was added at 20 % (w/w) to the mixture and re-stirred. Liquid matrix was packed in a syringe and added dropwise into a sterile solution of calcium chloride (CaCl_2) at 0.1 mol.L^{-1} (Nisco Encapsulator Unit Var1). The resulting beads were rein-

forced by stirring for 15 min in the CaCl_2 solution. Afterwards, CaCl_2 bath was replaced by sterile distilled water for 15 min in order to wash the beads. Finally, beads were filtered and immediately used.

Cells suspensions: a free cells solution was also prepared with phosphate buffer saline (PBS) and 20% (w/w) cells-glucose solution.



Survival of free and encapsulated cells at low pH

Cells suspensions, gels and beads were subjected to a static *in vitro* gastric digestion in a simulated gastric fluid without enzymes at pH 1.8. Samples were removed at 0, 20, 40, 60, and 120 min to follow the survival of the LAB in acid medium.

Biopolymeric matrices were dissolved in PBS in order to release bacteria. Decimal dilutions were performed and then drops of 10 μL of the dilutions were plated in 20 mL of M17 agar. Plates were incubated at 30°C for 24h and Colony Forming Units (CFU) were counted.

Bile salt solution tolerance of free and immobilized bacteria

Bile salts solution tolerance of bacteria was evaluated using a procedure adapted from Kechaou et al (2013).

Confocal laser scanning microscopy (CLSM)

Microstructures of gels were observed by confocal laser scanning microscopy (CLSM). Protein was stained with Rhodamine B Isothio cyanate (RITC) to localize the caseinate phase in the biopolymeric gels, and Syto@9/Propidium

iodide was used to localize probiotic LAB cells using the procedure described in Léonard (2016). Observation was performed with a 543 nm excitation wavelength and an emission wavelength range between 560 nm and 590 nm.

RESULTS AND DISCUSSION

Survival of free and encapsulated cells at low pH

Figure 1 shows that encapsulation (beads and gel) improved protection of bacteria in a pH 1.8 gastric medium in comparison of non-immobilized cells for the same time of incubation. It seems that Alg-Cas matrix would be effective to maintain LAB viability. It can be explained by the buffering capacity of caseinate which decreased the impact of the acidity combine with physical protection effect due to the polymers (Léonard, 2013).

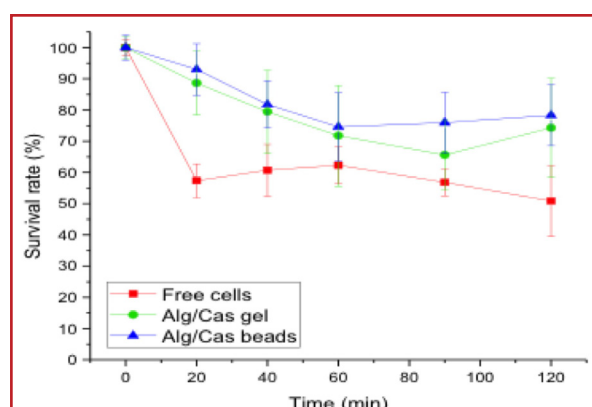


Fig 1: Cultivability of *Lc. Lactis Elafin* free and encapsulated in biopolymeric matrix during exposure to simulated gastric fluid without enzymes at pH 1.8

Bile salt solution tolerance of free and immobilized bacteria

The resistance of each strain to bile salt stress was determined using the growth delay (i.e. delay of time to reach mid-exponential phase) between stressed and non-stressed cultures. Figure 3 shows that the growth delay caused by the exposure to a bile salts solution was significantly reduced when bacteria were encapsulated in the Alg-Cas gels. (*Lb.* strains: controls)

Localization of LAB in biopolymeric matrix

LAB was stained to study their par-

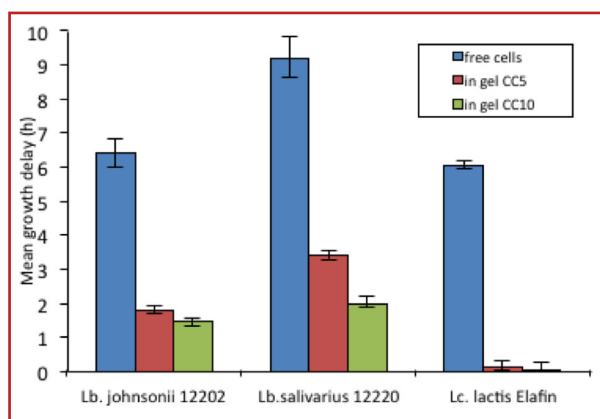


Fig 3: Bile salt tolerance of free and immobilized LAB strains in Alg-Cas gels. *Lactobacillus salivarius* VEL12220 and *Lb. johnsonii* VEL12202 were chosen as reference for their sensibility to bile salts (Kechaou, 2013).

tition in the self-gelled matrices: *Lactococcus lactis* cells were localized in protein micro-domains. Preferential partitioning of bacterial strains can be explained by a predominance of hydrophobic interactions and by considering that the salt and electrostatic contributions were similar between the two phases (Léonard et al, 2016).

CONCLUSIONS AND PERSPECTIVES

To conclude, Alg-Cas matrix seems to be a good system to encapsulate probiotic LAB and protect them against the acidity of gastric medium and bile salts solution. The results demonstrated that *Lc. lactis* cells had more affinity to caseinate than to alginate. This preferential localization in protein domains

enhanced the protection by chemical (buffering capacity) and physical effects.

To go further, the survival of free and encapsulated cells will be followed during an exposure at pH 1.8 in a simulated gastric fluid with digestive enzymes to determine the resistance of the cells to a new source of stress. Then cells will be transferred in an intestinal fluid at pH 6.5 during 2 hours where LAB cultivability will be followed at different times as well as Elafin production.

Finally, *Lc. lactis* Elafin will be subjected into a dynamic *in vitro* digester where the survival during GI digestion

will be evaluated as well as the release of Elafin in the intestinal tract.

REFERENCES

- Kechaou N., Chain F, J.J. Gratadoux , et al Appl. Environ. Microbiol. 79 (2013)
- P. Motta, Bermúdez-Humarán L-G, Deraison C., et al, Sci. Transl. Med. 4 (2012)
- Léonard L., Husson F., Langella P., Jean-Marc Châtel J-M., Saurel R, Colloids and Surfaces : Bio interfaces 141 (2016)
- Léonard L; Beji O., Arnould C. et al , Food Control 47 (2015)
- Léonard L; Gharsallaouia A, Ouaalila F., et al, Colloids and Surfaces B: Bio interfaces 109 (2013)

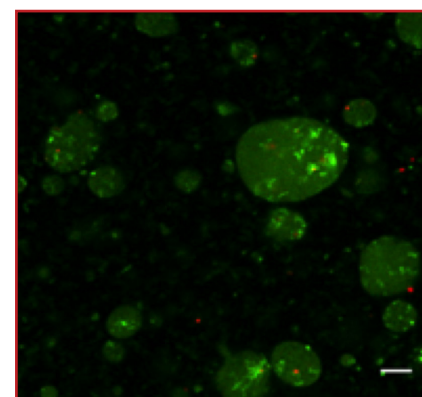


Fig 2: Confocal laser scanning microscopy observations of gelled alginate-caseinate (1.5–4 wt %) matrices with 10 mM calcium carbonate and *Lc lactis Elafin* (Cells stained with the live/dead BacLight® viability kit) (scale bar 10 µm).



Julie Chanut
Agrosup - Dijon
UMR PAM
Dijon, France
julie.chanut@agrosupdijon.fr

BRG 2018 MEETINGS

21TH MICROENCAPSULATION INDUSTRIAL CONVENTION



MONTREAL, PQ, CANADA - MAY 21-24, 2018

More information :

<http://bioencapsulation.net/2018-Montreal-Microencapsulation-Industrial-Convention/>

10TH TRAINING SCHOOL ON MICROENCAPSULATION



TRONDHEIM, NORWAY, SEPTEMBER 2018

More information, [web site will be available in January 2018](#)

BRG STEERING COMMITTEE

- **Prof. Denis Poncelet**, Oniris, France (President)
- **Prof. Stephan Drusch**, TU Berlin, Germany (Secretary)
- **Dr Corinne Hoesli**, McGill University, Canada (Secretary)
- **Prof. Ronald J. Neufeld**, Queen's University, Canada (Treasurer)
- **Prof. Paul De Vos**, Groningen University, Netherlands (Newsletter editor)
- **Mrs Brigitte Poncelet**, Impascience, France (Event manager)

-
- **Dr André Brodkorb**, Teagasc Food Research Centre, Ireland (Editor)
 - **Dr Thorsten Brandau**, Brace GmbH, Germany
 - **Prof. Berit Strand**, NTNU, Norway
 - **Prof. Francisca Avecedo**, and **Monica Rubilar**, Univ. Frontera, Chile
 - **Prof. Igor Lacik**, Polymer Institute, Slovakia
 - **Prof. Marijana Dragosavac**, Loughborough Univ. UK
 - **Prof Paola Pittia**, Teramo Univ. Italy
 - **Prof Herley Casanova**, Antioquia Univ. Colombia.
 - **Dr Claudia Preininger**, AIT, Austria
 - **Thierry Vandamme**, Strasbourg Univ. France
 - **Prof. Elena Markvicheva**, Institute of Bioorganic Chemistry, Russia
 - **Prof Luis Fonseca**, Instituto Superior Técnico, Portugal
 - **Dr James Oxley**, SwRI, USA
 - **Dr Amos Nussinovitch**, Hebrew University. Israel
 - **Dr Laura Hermida**, NITI, Argentina
 - **Mrs Catarina Silva**, FFUL, Spain.

REGISTRATION FORM (YOU MAY ALSO REGISTER ON [HTTP://BIOENCASULATION.NET](http://BIOENCASULATION.NET))

Bioencapsulation Research Group is a non-profit association promoting networking and research in the encapsulation technology of bioactives. It organises academic conferences and industrial symposiums, publishes newsletters and manages a website.

- Title: Registration class: Industrial / Researcher / Student
- First name: Last name:
- Affiliation: Department:
- Address: Address (cont.):
- Zipcode: City:
- State: Country:
- Phone: Email:

Send it to : Bioencapsulation Research Group 114 Allée Paul Signac, 44240 Sucé sur Erdre France or contact@bioencapsulation.net